How to quantify the cooling effects of green infrastructure strategies from a spatio-temporal perspective: Experience from a parametric study

Wanlu Ouyang [a,c,d,*], Tobi Eniolu Morakinyo [b], Yilin Lee [a,c], Zheng Tan [d,e,c], Chao Ren [f], Edward Ng [a,c,g]

[a] School of Architecture, The Chinese University of Hong Kong, Hong Kong, China
[b] School of Geography, University College Dublin, Ireland
[c] Institute of Future Cities, The Chinese University of Hong Kong, New Territories, Hong Kong, China
[d] Department of Building and Real Estate, The Hong Kong Polytechnic University, Hong Kong, China
[e] Research Institute for Smart Ageing, The Hong Kong Polytechnic University, Hong Kong, China
[f] Division of Landscape Architecture, Department of Architecture, Faculty of Architecture, The University of Hong Kong, Hong Kong, China
[g] Institute of Environment, Energy and Sustainability, The Chinese University of Hong Kong, New Territories, Hong Kong, China

HIGHLIGHTS

- Proposed a systematic approach to quantify the cooling effects of green infrastructure (GI) strategies.
- Proposed three indicators to assess the cooling effects from a spatio-temporal perspective.
- Compared the cooling effects of seven GI strategies based on three GI typologies.
- Investigated the impacts of urban morphology on the cooling provision of GI strategies.

GRAPHICAL ABSTRACT
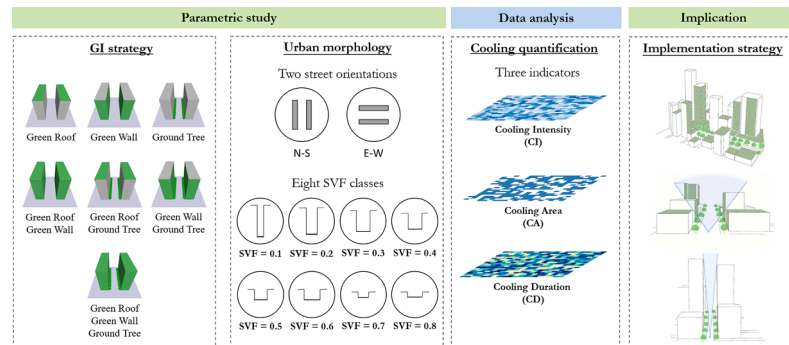
ARTICLE INFO

ABSTRACT

Urban green infrastructures (GI) are efficient nature-based solutions for urban heat mitigation. Typically, three GI typologies, i.e., green roof, green wall, and street tree, are often recommended and implemented for outdoor thermal comfort modification and passive energy saving. However, the current evaluation of the cooling effects for GI strategies is not comprehensive for two reasons: 1) lacking a holistic assessment to involve different combinations of GI typologies; 2) lacking a spatio-temporal lens to quantify the cooling effects.

This study proposes a systematic approach to quantify the cooling effects of GI strategies from a spatio-temporal perspective. Through a parametric study in ENVI-met model, the cooling effect of seven GI

---

strategies were quantified, and different street orientations and sky view factor (SVF) were also involved. Three cooling indicators were proposed for different sustainable planning targets: cooling intensity (CI), cooling area (CA), and cooling duration (CD). The results showed that the seven GI strategies performed differently under various urban morphologies. The greatest cooling effect of GI strategies was observed at SVF = 0.7, after which additional strategies may be needed for urban heat mitigation. Three proposed indicators were found to show similar patterns across the GI strategies, but revealed the details of cooling effects differently.

Overall, this study represents the first assessment of the cooling effects of seven GI strategies across different morphological settings. The evidence-based understanding contributed by this study can help planners and designers to optimize the thermal environment in subtropical climate. The systematic approach from a spatio-temporal lens can be transferred to other cities and climate backgrounds.

1. Introduction

1.1. Green infrastructure strategy for urban heat mitigation

The sixth Assessment Report released by the Intergovernmental Panel on Climate Change (IPCC) in 2021 indicates that human activities are unequivocally warming the environment, creating an irreversible trend usually occurring on the timescales of centuries (IPCC, 2021). As the hot extremes are becoming intensified, frequent and prolonged, tackling urban heat becomes a big concern for the many governmental authorities and policymakers. Therefore, it requires an innovative combination and implementation of passive and technological solutions for urban heat mitigation. In recent decades, green infrastructure (GI) has been widely advocated by policymakers and climate action planners as an effective strategy to adapt cities to urban heat (Ruth et al., 2017). For instance, London aimed to be the world's first National Park City in 2019, with the ultimate goal of turning 50% of the urban area green by 2050 (London Government, 2015). Additionally, Singapore has released the Green Plan 2030 to promote the planting of 1 million more trees for sustainable living (Singapore Government, 2021), and Hong Kong has published the Climate Action Plan 2050 to emphasize the application of GI in more effective places (HK Government, 2021).

GI can be classified into various typologies based on different criteria (Wong et al., 2021), e.g., deciduous and evergreen based on leaf life span (van Ommen Kloeke et al., 2012). In terms of implementation location, common GI typologies include green roof (intensive and extensive depending on the vegetation height and substrate depth), green wall (green façade and living wall differentiated by planting styles), and ground-level trees (street trees, park/ green space trees) (Ouyang et al., 2021, masked for blind review). These three GI typologies are widely used for microclimate regulation. However, to fully utilize the cooling potential of GI, it is necessary to understand the cooling effects of different GI strategies (based on various combinations of GI typologies) and their performance in different urban contexts from a holistic perspective (Norton et al., 2015).

To quantify the cooling effects of GI, remote sensing technology, field measurement, and numerical simulation are often used. Satellite images are widely employed to measure the land surface temperature and the impact of urban greening (Weng, 2009), but they are limited to representing the atmosphere conditions, thus cannot indicate thermal perceptions at the pedestrian level. Field measurement can be used to record the events and phenomena in reality through an instrument, but it does not enable sufficient experimental control for investigating "what-if" scenarios and presents potential uncertainties (i.e., pedestrians block the incoming shortwave and alter wind conditions (Liu et al., 2022; Stewart, 2011)). Numerical models are gaining popularity due to their advantage in isolating certain processes in the complex urban system (Arnfield, 2003); therefore, numerical models are applied and discussed in this study.

1.2. Necessity of a holistic assessment for the cooling effects of different GI strategies

In existing studies based on the numerical simulation method, the

pedestrian-level cooling effects of different GI typologies have been quantified separately. Regarding green roof, previous studies investigated the cooling effects of green roof at the pedestrian level and its features (i.e. green roof type (Morakinyo et al., 2017), coverage ratio (Jin et al., 2018; Morakinyo et al., 2017), layout (Jin et al., 2018; Zhang et al., 2019), and plant characteristics (i.e., Leaf area index – LAI) (Berardi, 2016)). These studies revealed that green roof reduced the air temperature (AT) by 0.05–0.6 °C at the pedestrian level (1.5–1.8 m above the ground), and the cooling effects were positively correlated with LAI of the plants and the greenery coverage ratios. For green wall, the cooling effect was influenced by different coverage ratios (Morakinyo et al., 2019; Wong et al., 2009), planting height and location (Acero et al., 2019), and plant shading coefficients (Wong et al., 2009). These simulation studies showed that green wall can cool the ambient environment and improve thermal comfort by decreasing air temperature (AT) by 1 °C and physiological equivalent temperature (PET) by 0.1–10 °C within 3–5 m from the walls. Trees are the most efficient GI for heat mitigation, which is often quantified in terms of the tree cooling intensity (Ng et al., 2012; Ziter et al., 2019) and cooling efficiency (Ouyang et al., 2020, masked for blind review), species selection (Kong et al., 2017; Z. Liu et al., 2020; Morakinyo et al., 2018), planting location and layouts (Ng et al., 2012; Tan et al., 2016; Wu & Chen, 2017; Zhao et al., 2018), leaf characteristics (Fahmy et al., 2010), etc. These studies reconfirmed the cooling potential of trees, and revealed the dependence of cooling provision on proper tree species selection, planting arrangements, and coverage ratio allocation.

Some studies examined the cooling effects of two or the three GI typologies and analyzed either the individual (GI) or synergistic effects, although this evidence is limited. For instance, in Munich, Germany, the cooling capacity of three GI typologies were compared, and trees showed the highest cooling potential, providing a 1 °C reduction in AT and a 13%–15% decrease in extreme heat; green roof showed no apparent heat mitigation, and green wall reduced PET by 4 % within a 2 m distance (Zölch et al., 2016). In Malda, India, green wall and green roof were investigated, and the results showed that combining green wall and green roof reduced the temperature by 1.29 – 1.87 °C (Ziaul & Pal, 2020). In Spain, combining trees, grass, and green roof reduced PET by up to 10 °C (Lobaccaro & Acero, 2015). In Sri Lanka, trees, green roofs, green walls, and the combination of all of them lead to AT reductions of 1.87 °C, 1.79 °C, 1.86 °C, and 1.9 °C respectively at the hottest hour (Herath et al., 2018). These results highlight the merits of combining GI strategies, as combining different GI typologies led to higher cooling effects than applying a single GI typology. Although the cooling effects provided by single or certain combinations of GI typologies can be extracted from different studies in the literature, it is warranted to analyze these effects within a singular study for unbiased comparative analysis and, ultimately, the development of evidence-based implementation strategies.

1.3. Significance of a spatio-temporal lens for GI cooling effects

In previous studies, the cooling effect has mostly been quantified by the differences between the GI and the corresponding bare/ reference scenarios, which is usually referred to as the cooling intensity (CI). CI is
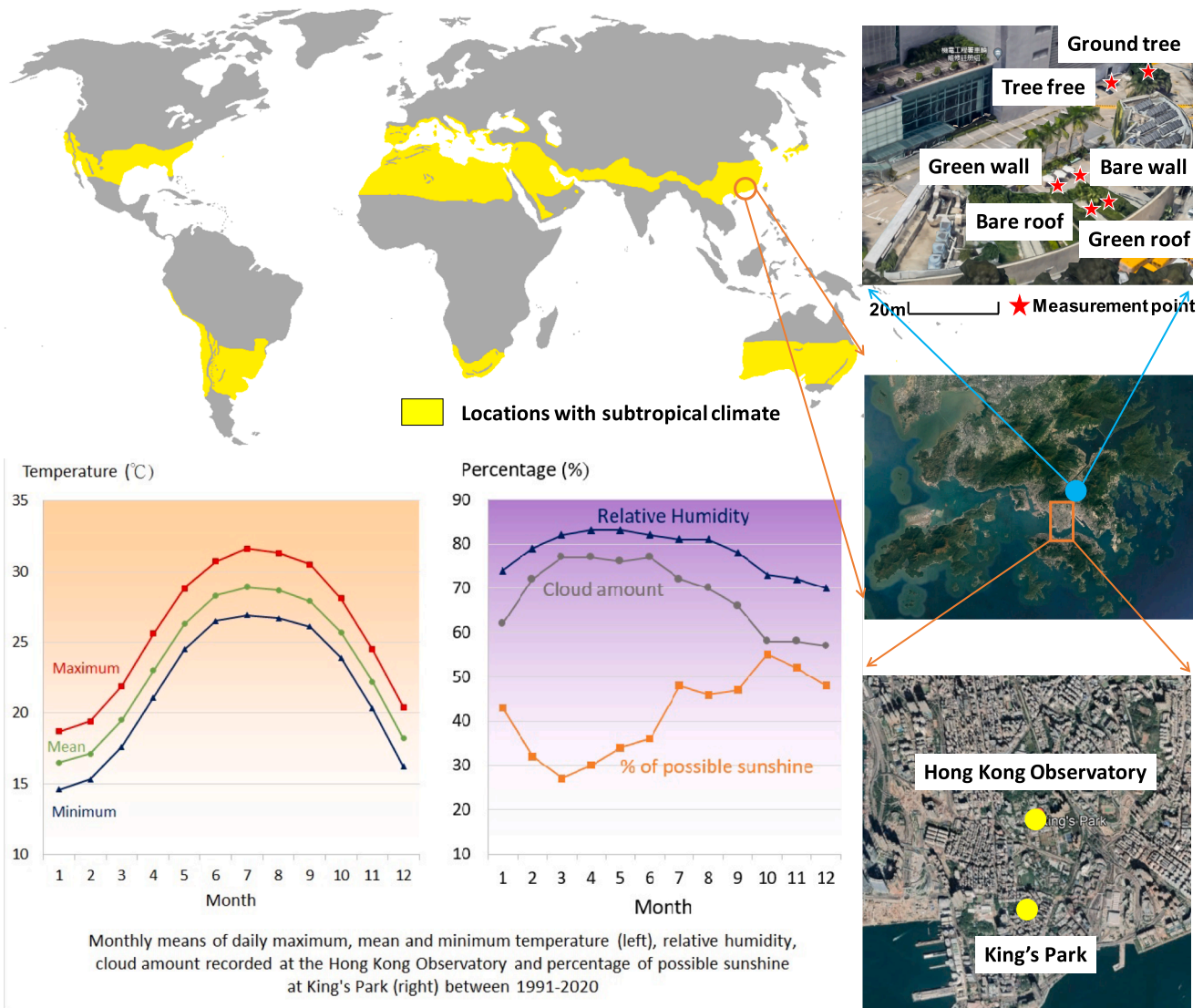
Fig. 1. HK and the basic climate graph (*Source: HKO website, Google map*).

often quantified by calculating the spatial (i.e., targeted analysis domain) and temporal (specific hour or a certain period) average of the chosen microclimate indicator. However, the average values may obscure the details of the spatial spread of cooling and the effective duration of the cooling effects.
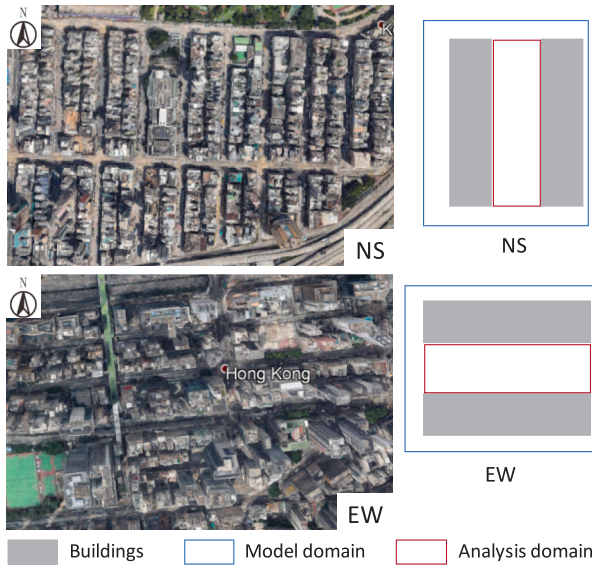
In the current literature, there are mainly four ways to present the spatio-temporal patterns in simulation or parametric studies: 1) showing the distributions of CI values, i.e., by boxplot (Ouyang et al., 2020, masked for blind review, Yin et al., 2019); 2) mapping the microclimate variables with the aid of Leonardo in ENVI-met (Lan et al., 2021; Tan et al., 2022); 3) presenting the frequency distribution of CI values from a temporal perspective, i.e., by ridge plot (Ouyang et al., 2020, masked for blind review, Qin et al., 2021); and 4) visualizing the spatio-temporal average values for different cases and hours, i.e., by heatmap (Rodrí-guez Algeciras et al., 2016; Rodríguez-Algeciras et al., 2021). The above methods describe the data distributions from different perspectives, including value dispersion, spatial patterns, and temporal variation. Therefore, these methods can support the understanding of how temperature varies across different locations and times. However, they do not directly show the specific effective areas or cooling periods, which would be useful to support policy-makers to formulate guidelines or thresholds for urban planning and design processes. Therefore, it is necessary to develop a proper indicator that provides a spatio-temporal

perspective and, thus directly shows policymakers the efficiency of a certain strategy in terms of how many areas can be affected and how long periods of these effects.

1.4. Impacts of urban morphology on microclimate and GI cooling

In the field of climate-sensitive planning and design, urban morphology is a significant factor to be considered. A street canyon is, a basic geometric unit in urban areas, consisting of two rows of buildings and the space between them (Oke, 1988), and the geometry of street canyons has been shown to play an important role in the microclimate and outdoor thermal comfort (Jamei et al., 2016). The geometry of street canyons is widely quantified by street orientation and sky view factor (SVF). Specifically, SVF is a dimensionless parameter ranging from zero to one that measures the percentage of unobstructed sky seen from a target location (Gong et al., 2018). Lower SVF values can lead to lower AT in the daytime and higher AT at night (Unger, 2004). Street orientation, which describes how buildings and canyons are oriented, can affect the amount of solar access and the wind speed in the canyons, subsequently impacting pedestrian thermal comfort on a typical summer day (Ali-Toudert & Mayer, 2006) and the length of the sun exposure period (Acero et al., 2021). For example, East-West (EW) oriented streets are exposed to solar radiation for longer than North-South (NS) oriented

(a) Street orientation

(b) Sky view factor

Model	SVF	Height (m)	Width (m)	AR (H/W)
H60W12	0.1	60	12	5.00
H50W20	0.2	50	20	2.50
H40W26	0.3	40	26	1.54
H30W26	0.4	30	26	1.15
H20W24	0.5	20	24	0.83
H20W30	0.6	20	30	0.67
H10W20	0.7	10	20	0.50
H10W28	0.8	10	28	0.36

$y = 0.3399x^{-1.219}$
$R^2 = 0.9846$

SVF = 0.1 SVF = 0.5
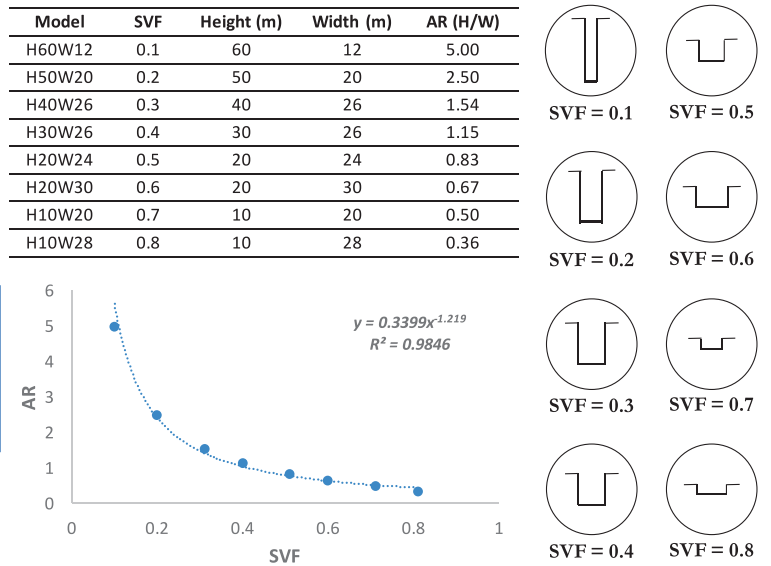SVF = 0.2 SVF = 0.6
SVF = 0.3 SVF = 0.7
SVF = 0.4 SVF = 0.8

Fig. 2. Illustration of the urban morphology scenarios.

streets, thus meaning the former show low thermal comfort levels (Johansson, 2006)..

In terms of the impacts of urban geometry on GI cooling, a study revealed that, when applying both green wall and green roof, minor differences were found between NS and EW orientations (0.1 °C for daytime average), but the difference became more significant for green wall only (0.8 °C) (Alexandri & Jones, 2008). In the same study, the impacts of aspect ratios were also explored, which indicated that green roof and green wall had a weaker cooling effect in wider canyons (Alexandri & Jones, 2008). However, this pattern was not the same for tree strategy, as the street tree was more effective in EW oriented streets (Yin et al., 2019). Additionally, for the compact canyons, trees provided lower cooling effects because the high buildings provided enough shading (Ng et al., 2012; Ouyang et al., 2020, masked for blind review). A recent study proposed a tree selection approach based on SVF (Morakinyo et al., 2020), as canyons with different geometries had varying thermal conditions (Tan et al., 2016, 2017). The above evidence confirms the impacts of urban geometry on GI cooling provision, but these impacts were reported in different studies with various site settings and background climates, thus hindering the direct cross-comparisons. Therefore, it is necessary to systematically explore the impacts of urban geometry when implementing GI strategies in local contexts.

1.5. Research gaps and objectives

Three research gaps can be identified in the existing literature. Firstly, previous studies have predominantly focused on examing the cooling effect of a single GI typology or directly comparing a single GI typology with combined GI typologies. Therefore, little is known about the differences in the cooling effects of GI strategies, especially for various combinations of GI typologies. Secondly, the cooling effects have mainly been described in terms of the average values of the analysis area at the hottest hour. Consequently, it is warranted to measure the cooling effects from a spatio-temporal perspective. Thirdly, it is worth investigating the cooling performance of GI strategies in different morphological conditions.

Therefore, this study aims to provide a systematic quantification of the cooling effects of GI strategies from a spatio-temporal perspective. Based on a validated ENVI-met model, a parametric study was conducted for seven GI typologies, two street canyon orientations, and eight SVF classes. Thereafter, the cooling effects at the pedestrian level were

quantified in terms of three cooling indicators: cooling intentisty (CI), cooling area (CA), and cooling duration (CD). Three objectives were achieved: 1) comprehensively estimating the thermal-radiant performance of seven GI strategies; 2) proposing three cooling indicators to quantify the cooling effects from a spatio-temporal perspective; 3) systematically examining the impacts of urban morphology on the cooling provision of the GI strategies. This study can inspire future parametric studies regarding the comprehensive quantification of GI cooling effects, as the evaluation approach and proposed indicators can be applied to other sites and cities. The findings of this study also provide a spatio-temporal lens to support urban planners to select the appropriate GI strategies based on the urban morphology of their design site.

2. Methodology

2.1. Study area and its representativeness

Hong Kong (HK), located on the southeast coast of China (22.32° N, 114.17° E), has a humid subtropical climate (*Cfa*) according to *Köppen* climate classification system (Fig. 1). The summer months range from June to September, with average daily temperatures of 28.4–30.2 °C and a relative humidity of 73–84 % (HKO, 2019, 2020). As a representative city for the (sub)tropical climate, HK has been making efforts in climate action to develop climate-resilient cities (Ng et al., 2012). In the last 2 decades, the HK government has released several policies regarding urban greening to improve the thermal environment on a scale from the city to buildings. For instance, the Green Master Plan (GMP) provides an overall greening framework for specific urban districts (Hong Kong Civil Engineering and Development Department, 2004), the Planning Standards and Guidelines suggest 30% green coverage for new public house development (Planning Department, 2010), and the Practice Note APP-152 provides guidelines for gross floor area and site coverage calculation for the implementation of greening in new building development (Buidling Department, 2016).

2.2. ENVI-met model and validation

The parametric study presented in this paper was conducted in ENVI-met — a holistic, 3D, non-hydrostatic model. This model can simulate the complex interactions among surfaces, plants, and atmosphere (Huttner, 2012), and thus is one of the most widely used microclimate
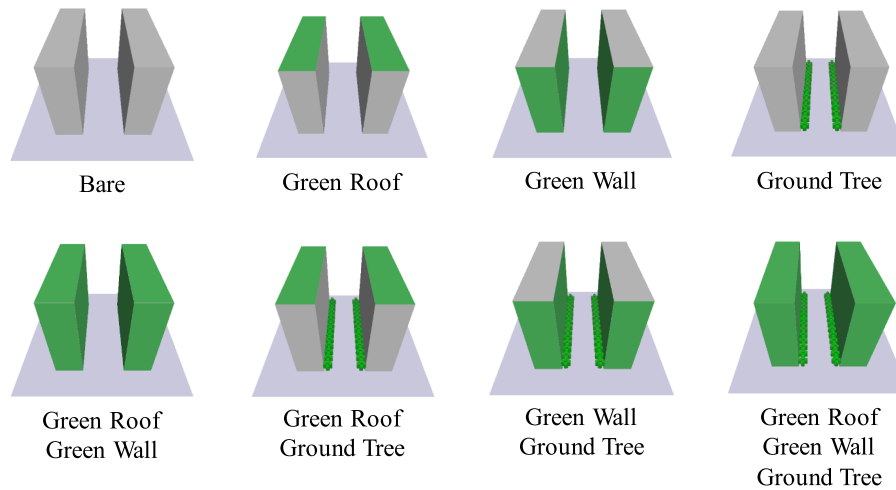
Fig. 3. Illustration of the GI scenarios.

models to investigate the relationship between urban greening and urban morphologies (Tsoka et al., 2018). ENVI-met can estimate the microclimatic variations on both the spatial and temporal levels, with high spatial (0.5–10 m) and temporal (1–5 s) resolution. Recently, ENVI-met V5 incorporated a 3D vegetation module to mimic complex vegetation geometries, which has improved the estimation accuracy for urban greening by considering plants as biological and dynamic bodies and involving evapotranspiration and energy absorption in the simulation (Simon et al., 2020).

Based on field measurement data, the performance of ENVI-met was validated for the three GI typologies, namely green roof, green wall, and ground tree. To achieve this, the thermal-radiant variables were collected during typical summer days in the courtyard of the Electrical and Mechanical Services Department (EMSD), where three GI typologies are present. The measurement equipment and process were illustrated in our earlier study (Ouyang et al., 2021, masked for blind review). Subsequently, using ENVI-met, the measurement site was modeled and the microclimate was simulated. The detailed model settings can be found in Table A1 in Appendix. Thereafter, the simulation results were evaluated in relation to the measurement data for three GI typologies (including six points — three GI and three reference points). The model validation results were presented in Table A2 in Appendix. The detailed evaluation processes were reported in our previous study (Ouyang et al., 2022, masked for blind review). In summary, the estimation accuracy of ENVI-met is reasonable for the three GI typologies, regardless of thermal and radiative variables, and, thus, ENVI-met can justifiably be applied for the following parametric studies and analyses.

2.3. Parametric study

2.3.1. Model configuration and urban morphology

The model domain consisted of two parallel buildings (building length × width: 20 m × 90 m), whose heights varied from 10 m to 60 m depending on different SVF scenarios. The grid resolution was 2 m × 2 m × 3 m to balance both simulation accuracy and efficiency (Salata et al., 2016). Additionally, 10 empty cells and 10 nesting grids were added to the lateral boundary to ensure simulation stability and minimize edge effects. The simulation was conducted for a typical summer day in HK with an air temperature of 28.48–33.15 °C and a relative humidity of 59.62–85.69%. It should be noted that in order to exclude the impact of wind conditions, this parametric study set the wind speed as static at 1 m/s for all hours (CUHK, 2008), and the direction was parallel to the street canyons. The semi-hourly inputs for full forcing can be found in our model evaluation study (Ouyang et al., 2022, masked for blind review).

Considering the complexity of urban morphology, especially in HK, a generalized and representative model was established based on real situations. As shown in Fig. 2. (a), two typical street canyon orientations (NS and EW) were modelled. Moreover, SVF, ranging from 0.1 to 0.8, indicated the openness or compactness of the urban morphology, with larger SVF values representing open canyons and smaller values indicating shallow and compact canyons. Based on Oke's method (Oke, 1988), eight SVF scenarios were built with different combinations of building heights (H) and street widths (W). Assuming the street canyon is infinitely long and symmetrical, the view factor of each wall can be calculated with equation (1)–(2), and then the SVF of both walls can be obtained through equation (3). Fig. 2. (b) presents the eight SVF cases, their H and W values and the correlation relationship between SVF and aspect ratio (AR, also known as H/W).

$$\varphi_w = (1 - \cos\theta)/2 \tag{1}$$

$$\theta = \tan^{-1}(H/0.5*W) \tag{2}$$

$$\varphi_s = (1 - (\varphi_{w1} + \varphi_{w2})) \tag{3}$$

2.3.2. GI scenarios and analysis domain

As shown in Fig. 3, eight scenarios were built, including one reference scenario (bare), three scenarios with a single GI typology (green roof, green wall, ground trees), three scenarios with two combined GI typologies (green roof + green wall, green roof + ground tree, green wall + ground tree), and one scenario with the three GI typologies combined (green roof + green wall + ground tree). These seven GI strategies are mentioned as Roof, Wall, Tree, RoofWall, RoofTree, WallTree, RoofWallTree respectively in the following text. This study mainly focused on the cooling effects of these seven GI strategies. The coverage ratios of green roof and green wall were set as 100%, and two rows of trees were planted within the street canyons at identical distances apart (8 m); therefore, the impacts of coverage ratios and planting configurations can be excluded. The characteristics of the greening were listed in Table A1.

2.4. Cooling indicators

Three cooling indicators were proposed to quantify the cooling effects of the GI strategies: cooling intensity (CI), cooling area (CA), and cooling duration (CD). In this study, CI measured the average cooling effects between the GI case and the corresponding reference case within the analysis area, CA quantified the percentage of the grids providing cooling effects above a certain threshold, and CD indicated for specific cooling periods (in hours), the cooling areas with cooling effects above a
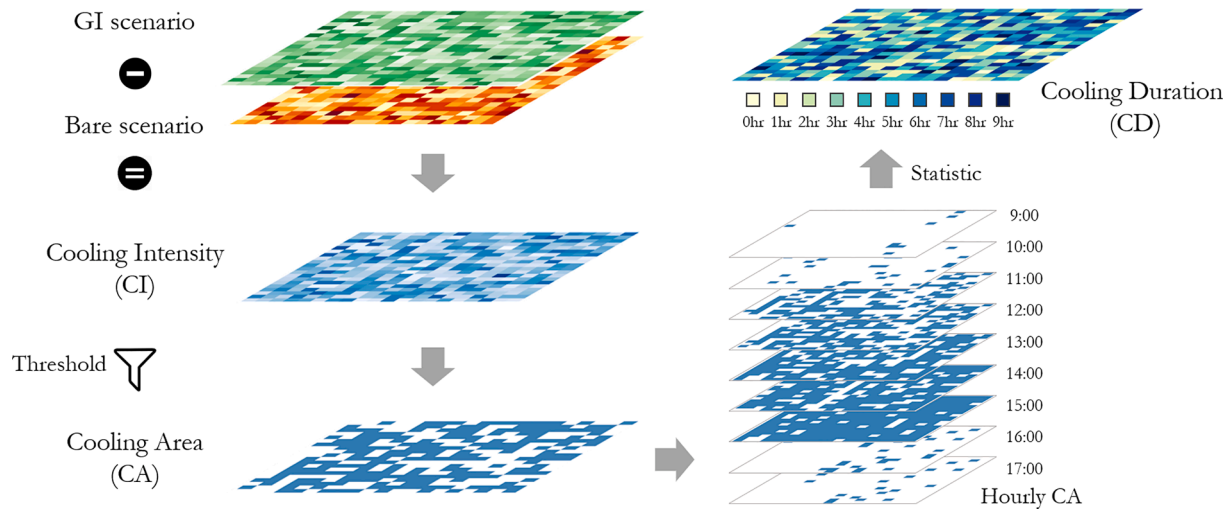
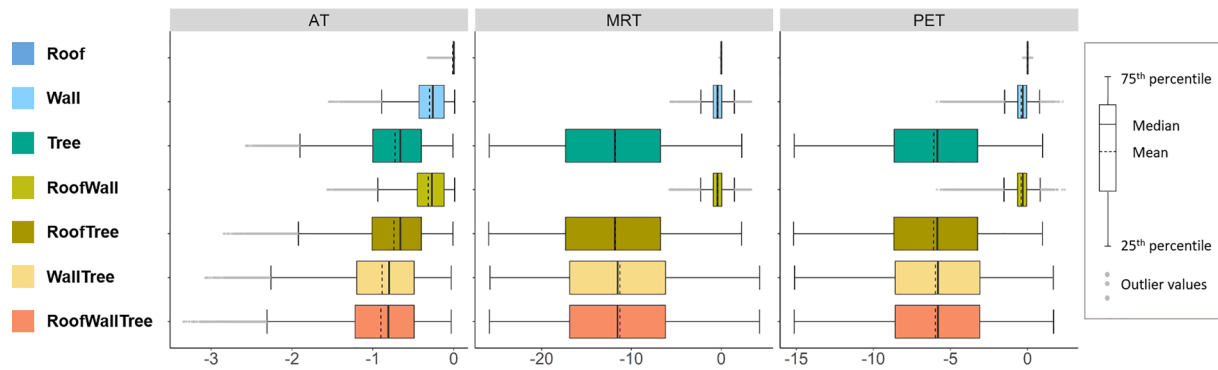**Fig. 4.** Illustration of the three cooling indicators.

Fig. 5. Cooling rankings of the seven GI strategies across three variables.

Table 1
The statistical results regarding the cooling performance of GI strategies (Unit: °C).

Variable	GI Strategy	Max	Min	Mean	Median	Std
AT	Roof	0.01	−0.32	−0.01	0.00	0.04
	Wall	0.01	−1.54	−0.30	−0.26	0.22
	Tree	−0.01	−2.57	−0.73	−0.66	0.42
	RoofWall	0.01	−1.56	−0.31	−0.27	0.24
	RoofTree	−0.01	−2.84	−0.74	−0.66	0.44
	WallTree	−0.03	−3.07	−0.88	−0.80	0.51
	RoofWallTree	−0.03	−3.34	**−0.90**	−0.81	0.53
MRT	Roof	0.01	−0.15	−0.01	0.00	0.01
	Wall	3.31	−5.65	−0.41	−0.42	1.09
	Tree	2.28	−25.85	−11.78	−11.85	6.45
	RoofWall	3.31	−5.74	−0.42	−0.43	1.09
	RoofTree	2.26	−25.91	**−11.79**	−11.85	6.45
	WallTree	4.26	−25.75	−11.28	−11.54	6.58
	RoofWallTree	4.25	−25.81	−11.28	−11.55	6.58
PET	Roof	0.29	−0.28	0.00	0.00	0.04
	Wall	2.28	−5.88	−0.41	−0.31	0.67
	Tree	0.97	−15.14	−6.09	−5.85	3.61
	RoofWall	2.40	−5.87	−0.42	−0.31	0.67
	RoofTree	0.96	−15.17	**−6.10**	−5.86	3.62
	WallTree	1.67	−15.11	−5.98	−5.81	3.66
	RoofWallTree	1.68	−15.13	−5.99	−5.81	3.67

certain threshold. CI focuses on the absolute cooling effects, whereas CA measures the spatial dispersion of the cooling effects, and CD measures the cooling duration and dispersion in spatial and temporal perspectives. The cooling effects in this study refer to the value differences between

the GI case and the bare case (see equation (4)). These three indicators are calculated based on the equation (5)–(7). The illustration of these three cooling indicators can be found in Fig. 4.

Three thermal variables were considered and reported in this study: air temperature (AT), mean radiant temperature (MRT), and physiological equivalent temperature (PET). To differentiate the cooling effects of different GI strategies, the cooling thresholds for AT, MRT, and PET were set as 0.5 °C, 5 °C, 4 °C respectively. These settings were based on the previous references and ISO standards. Specifically, one earlier study found that the lowest mean AT change for the three GI typologies was about 0.5 °C (XXX et al., 2021, masked for blind review), the measuring accuracy requirement for the thermal stress level was ± 5 °C for MRT (ISO, 1985), and the PET change value for each thermal perception class was in the 4 °C range (Morakinyo et al., 2020).

$$CV_i = V_{GI i} - V_{Bare i} \tag{4}$$

$$CI = \frac{\sum_1^n CV_i}{n} \tag{5}$$

$$CA = \frac{Count(CV_i < V_{threshld})}{n} \tag{6}$$

$$CD_{hr} = Hour\left(\frac{Count(CV_i < V_{threshld})}{n}\right) \tag{7}$$

where CV_i is the cooling effect for the ith grid within the analysis domain, $V_{GI i}$ is the ith grid value of the GI case; $V_{Bare i}$ is the ith grid value of the corresponding bare case; $V_{threshold}$ is the threshold for a certain variable; Count() is the function to count the number of the grids; Hour()

Table 2
ANOVA results regarding the cooling performance of the seven GI strategies.

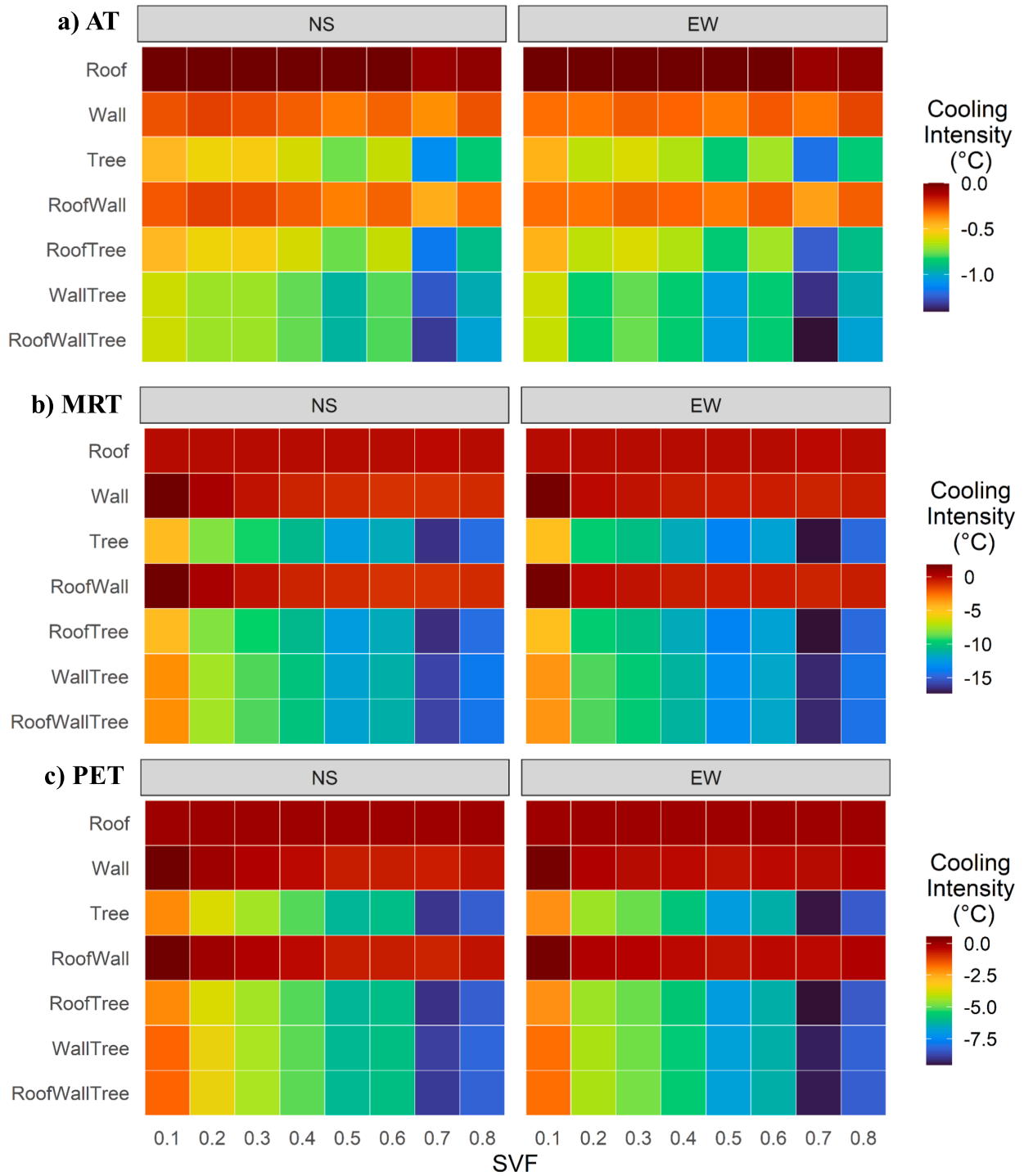| Variable		Df	Sum Sq	Mean Sq	F value	Pr (>F)
AT	GI	6	53,104	8851	60,329	< 0.001
	Residuals	527,303	77,359	0		
MRT	GI	6	16,383,949	2,730,658	110,940	< 0.001
	Residuals	527,303	12,978,996	25		
PET	GI	6	4,291,645	715,274	92,933	< 0.001
	Residuals	527,303	4,058,495	8		

Fig. 6. Cooling intensity (CI) of different GI scenarios across different urban morphology.
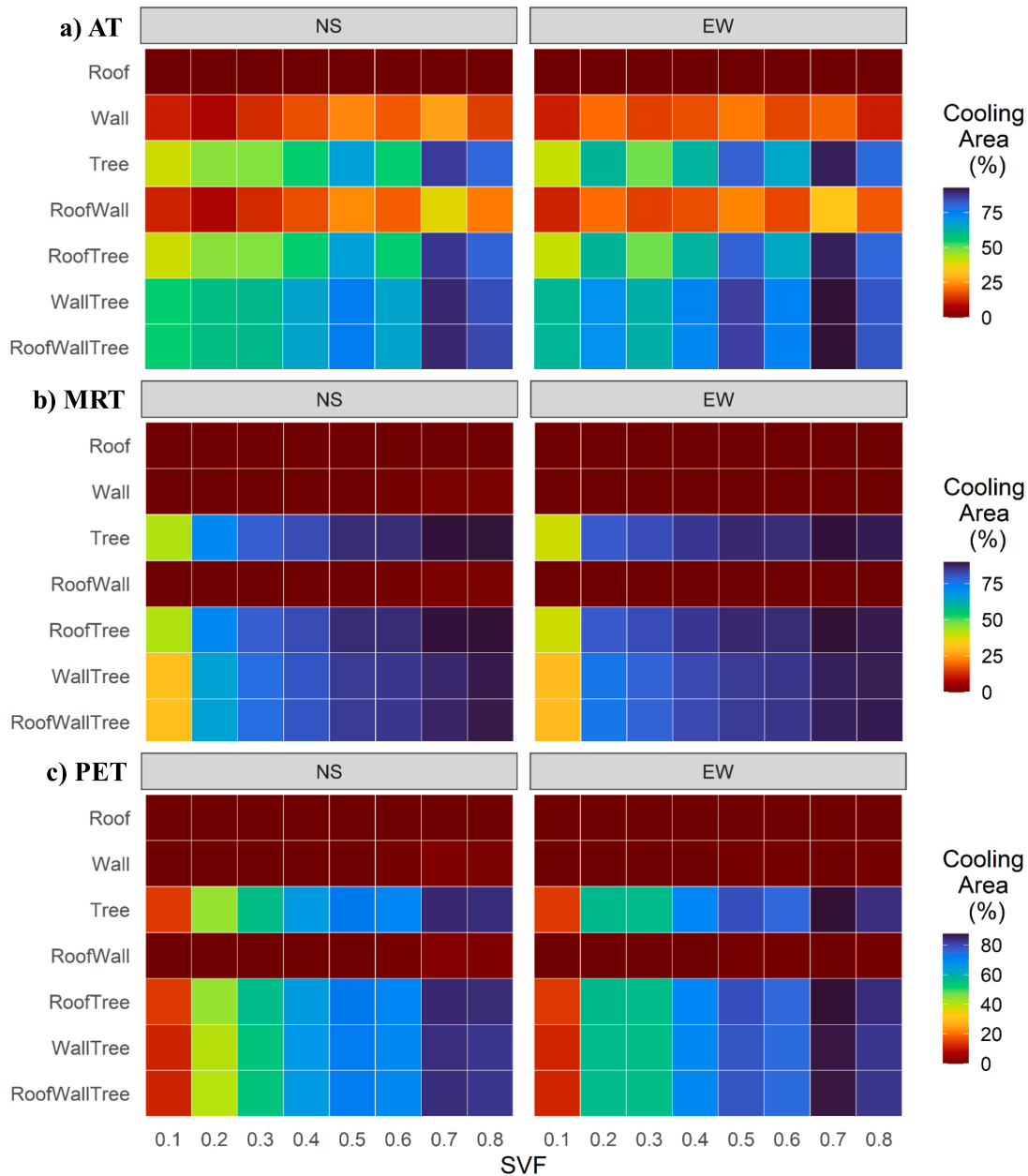
Fig. 7. Cooling area (CA) of different GI scenarios with different urban morphology.

is the function to identify the duration of the cooling effects; the unit of CI is degrees Celsius (°C); and the unit of CA and CD is percent (%).

3. Results

3.1. Ranking the overall cooling of the seven GI strategies

This section compares the cooling intensity of the seven GI strategies for the urban morphology cases with eight SVF scenarios and two orientation scenarios, all grids within the analysis domain (see Fig. 2), and all diurnal hours (9:00 – 17:00). As shown in Fig. 5, the cooling rankings of the seven GI strategies were dissimilar across the three thermal variables.Specifically, based on the average values, Roof had the lowest cooling effect, with nearly no cooling benefit for the pedestrian level regardless of the thermal variables. The RoofWallTree strategy provided the greatest reduction in AT(0.9 °C), while RoofTree decreased MRT and PET the most (11.79 °C and 6.10 °C). When

involving trees in the GI strategies, the cooling effects were greatly improved. For instance, Tree, RoofTree, WallTree, and RoofWallTree had cooling effects of 0.73 – 0.90 °C for AT, 11.28 – 11.79 °C for MRT, and 5.98 – 6.09 °C for PET. Additionally, for MRT and PET, certain GI strategies can lead to a warming effect (maximum value in Table 1). This indicates that some GI strategies should be carefully examined in relation to certain urban morphology before implementation. This also justifies the necessity of this study in terms of conducting a systematic evaluation of GI strategies across different urban morphologies. The details of the cooling performance of seven GI strategies can be found in Table 1.

In order to examine whether there is a significant difference between the cooling effects of seven GI strategies, a one-way analysis of variance (ANOVA) was conducted. As shown in Table 2, there were significant differences in the cooling performance between the GI strategies. Further post-hoc tests were applied to explore the comparisons between each pair. The results showed that all pairs of GI strategies presented
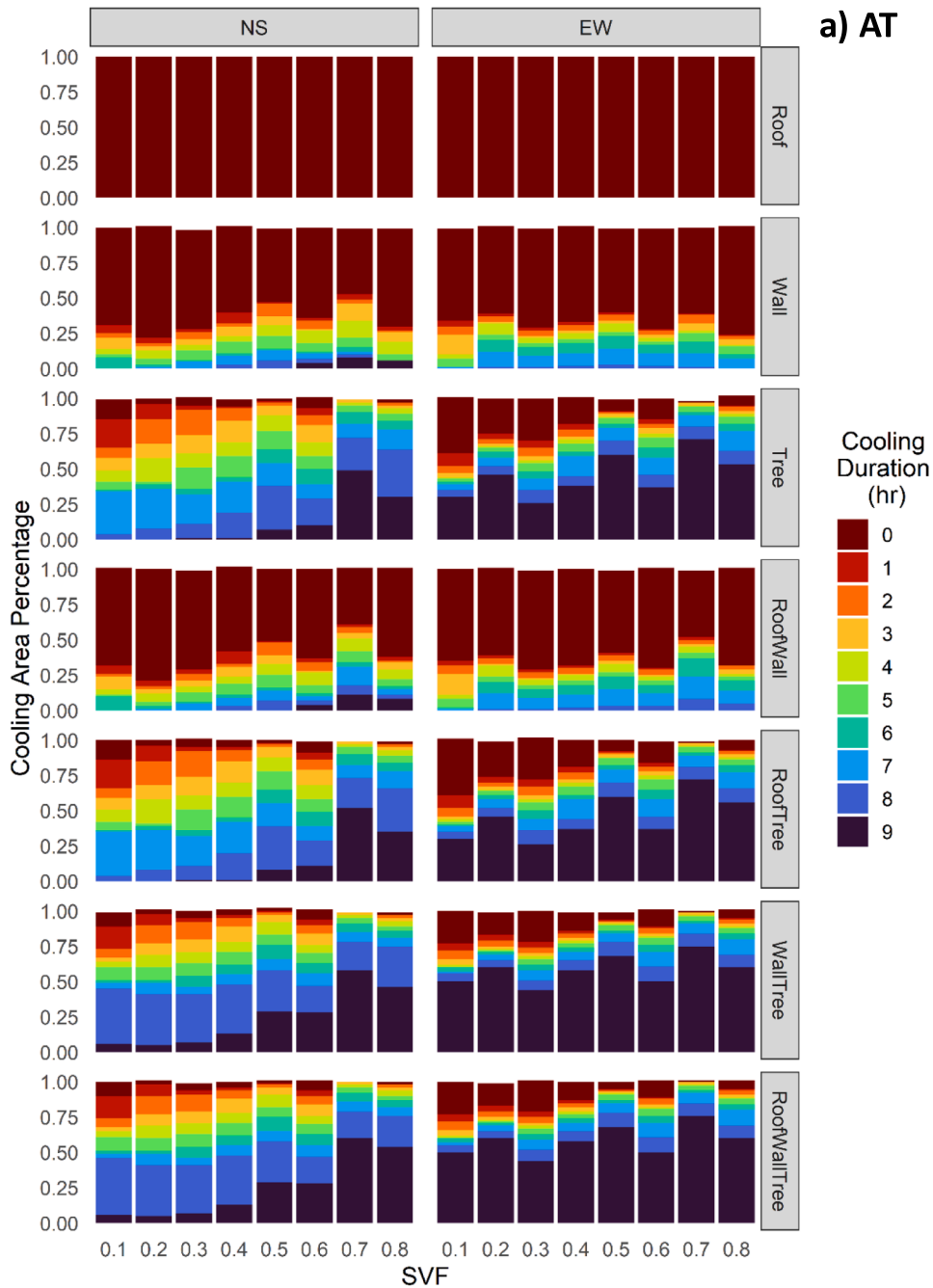
Fig. 8. Cooling duration (CD) of different GI scenarios with different urban morphology: a) AT, b) MRT, c) PET.

significant differences in terms of AT, indicating that different GI strategies influenced AT conditions variously. As for MRT and PET, Wall–RoofWall, Tree–RoofTree, WallTree–RoofWallTree showed non-significant differences regarding their cooling effects. These results indicate that the Roof strategy makes limited contributions to improving pedestrian thermal comfort. The detailed results are reported in Table A3 in the Appendix.

3.2. Cooling intensity of the seven GI strategies

Cooling intensity (CI), identified as the cooling difference between the GI case and the bare case, represents the average impact of a GI strategy in relation to a particular analysis domain. Lower CI values

indicate higher cooling effects, and vice-versa. As shown in Fig. 6, CI was affected by GI strategies and urban morphologies.

Across the seven GI strategies, RoofWallTree showed the largest AT reduction, while RoofTree presented the largest CI values for MRT and PET reduction. Irrespective of the type of thermal variable, the GI strategies implemented on building surfaces, namely Roof, Wall, and RoofWall, showed limited contributions to cooling (the greatest cooling was $-0.44\ ^{\circ}$C to $-0.07\ ^{\circ}$C for AT, $-1.12\ ^{\circ}$C to $-0.02\ ^{\circ}$C for MRT, $-0.76\ ^{\circ}$C to $-0.04\ ^{\circ}$C for PET). Additionally, Wall and RoofWall caused a slight increase in MRT (1.73–$1.84\ ^{\circ}$C) and PET (0.46–$0.54\ ^{\circ}$C) in street canyons with SVF $= 0.1$. One possible reason is that the impact of shortwave radiation was reduced, as limited solar radiation could penetrate into the deep canyon, so longwave radiation may have played an important
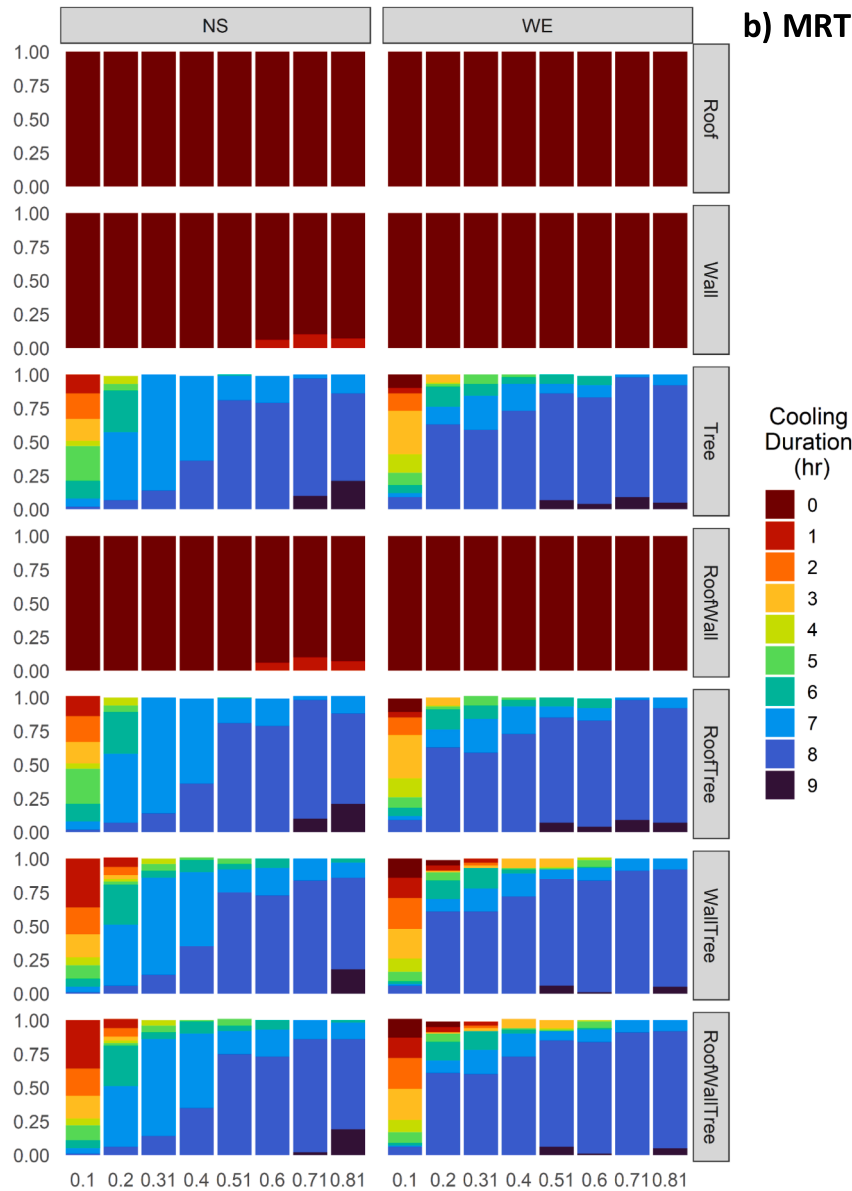
Fig. 8. (*continued*).

role. Another possible explanation is that the leaves exert drag effects on the wind environment, and lower wind speeds may lead to slightly higher MRT and PET values. When the GI strategies included trees, CI was greatly improved across all three thermal variables. For instance, the greatest cooling was −1.19 °C to −1.10 °C for AT, −17.30 °C to −16.49 °C for MRT, −9.03 °C to −9.50 °C for PET by Tree, while −1.41 °C to −1.32 °C for AT, −16.77 °C to −15.97 °C for MRT, −9.42 °C to −8.94 °C for PET was observed for RoofWallTree. Other details can be found in Table A4 in Appendix.

Regarding the impacts of urban morphology, although CI showed similar trends between the two orientations, EW-oriented streets showed higher CI values than NS orientations when implementing the GI strategy with trees. For example, when applying the Tree strategy, the CI difference between EW and NS orientations was −0.10 °C to 0.01 °C for AT, −1.43 °C to −0.16 °C for MRT, and −0.81 to −0.06 °C for PET, and the corresponding CI differences were −0.14 °C to 0.00 °C for AT, −1.48 °C to −0.14 °C for MRT, and −0.80 °C to 0.08 °C for PET when applying RoofWallTree. As for the impacts of SVF, the cooling effects were more

apparent with higher SVF. The highest cooling effects were achieved for canyons with SVF = 0.7; after that, the cooling effects were slightly lower with higher SVF values. Indeed, for RoofWallTree applied in NS-oriented canyons, the CIs at SVF = 0.7 and 0.8 were −1.32 °C and −1.02 °C for AT, −15.97 °C and −14.14 °C for MRT, and −8.94 °C and −8.29 °C for PET. This pattern was consistent across all the GI strategies and the two canyon orientations, whose details were reported in Table A4.

3.3. Cooling area of the seven GI strategies

Cooling area (CA) was calculated as the percentage of areas/ grids with cooling effects above certain thresholds. In this study, the threshold was set as 0.5 °C for AT, 5 °C for MRT, and 4 °C for PET. CA indicates the spatial effects of GI strategies, with higher CA values indicating larger impact areas of a GI strategy. As shown in Fig. 7, CA was closely related to both GI strategies and urban morphology.

From the seven GI strategies, RoofWallTree impacted the largest
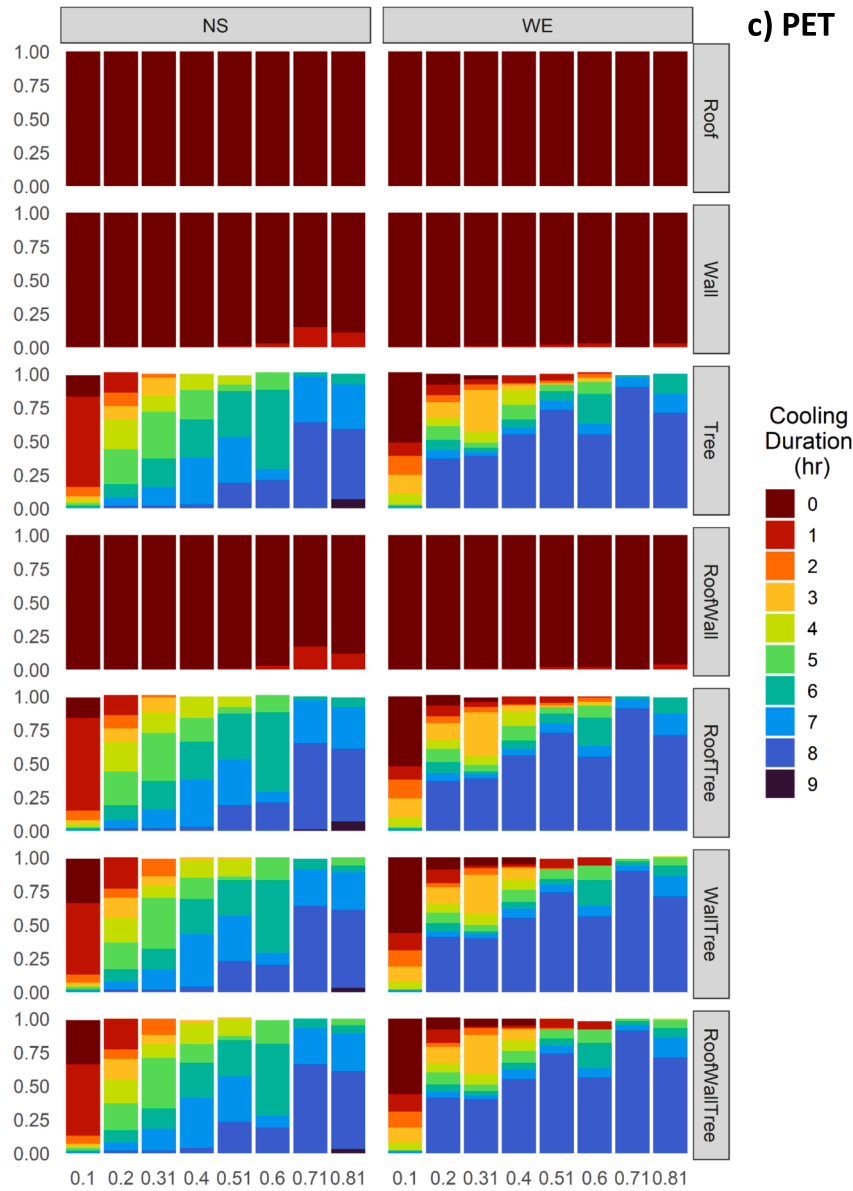
Fig. 8. (*continued*).

spatial domain in terms of AT reduction, while Tree and RoofTree showed the largest CA values for MRT and PET reductions. Similar to the CI indicators, the GI strategies targeting building surfaces (i.e., Roof, Wall and RoofWall), showed insignificant cooling areas for the three outcome variables. Specifically, with given cooling thresholds, Roof provided no cooling effects at the pedestrian level, and Wall and Roof-Wall only showed 7%–27% and 7%–38% cooling areas, respectively, for AT. And there was nearly no cooling areas for MRT and PET. This indicates that green wall moderates the ambient temperature near the walls through evaporation processes but has insignificant effects on the radiant environment. Trees greatly increased the cooling areas, indeed. For instance, for the Tree strategy, the CA was 41%–91% for AT, 40%–90% for MRT, and 14%–88% for PET. As for the RoofWallTree strategy, CA was 55%–93% for AT, 30%–89% for MRT, and 12%–87% for PET. Other details are revealed in Table A5 in the Appendix.

Concerning the urban morphology, the two street orientations showed similar patterns for CA. However, the EW-oriented canyons had higher CA values than those with NS orientation due to the higher solar exposure and thermal discomfort in EW orientations. The largest CA differences between the two orientations were 13%–14% for AT, achieved by the RoofWall, RoofTree, WallTree, Tree and RoofWallTree strategies. For MRT and PET, the largest differences were 8%–10% and 13%–16% respectively, for the RoofWall, WallTree, and RoofWallTree strategies. Regarding the SVF settings, higher CA was found in the canyons with higher SVF. Indeed, the largest CA values were identified in canyons with SVF = 0.7, and CA slightly decreased with SVF = 0.8. For example, for RoofWallTree, CA for AT was 90% in canyons with SVF = 0.7, but reduced to 85% with SVF = 0.8. This SVF pattern was constant across the two orientations and seven GI strategies. Please find the remaining details in Table A5.

3.4. Cooling duration of the seven GI strategies

Cooling duration (CD) is defined as the percentage area showing cooling effects (above the targeted threshold the same as for the CA calculation) for a certain number of hours, and this indicator considers

Fig. 9. Demonstration of the suggested strategies for different morphological conditions.

Table A1
Main settings of ENVI-met.

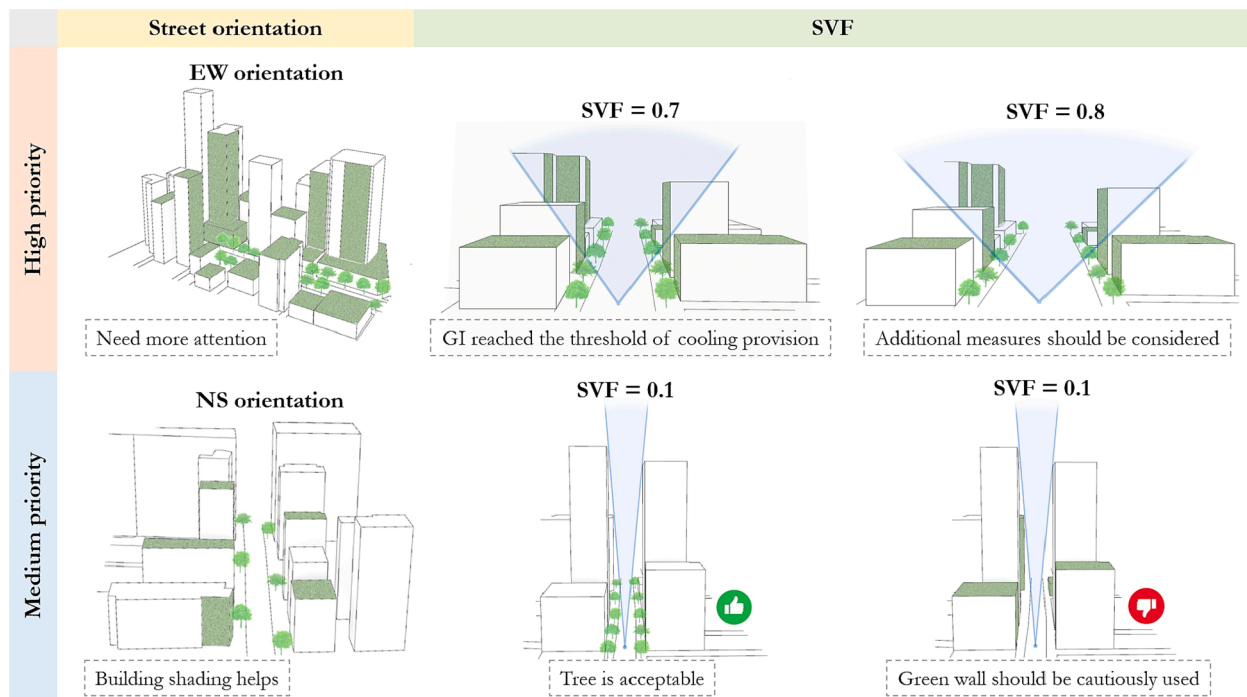| Construction & Plant	Input Parameter [Unit]	Settings
Ground pavement	Albedo	0.15
	Emissivity	0.9
Building roof	Thickness [m]	0.3
	Albedo	0.2
	Emissivity	0.7
	Thermal conductivity [W/(m.K)]	1.13
	Specific heat [J/(kg.K)]	1060
	Density [kg/m^3]	2225
Building wall	Thickness [m]	0.3
	Albedo	0.2
	Emissivity	0.9
	Thermal conductivity [W/(m.K)]	1.44
	Specific heat [J/(kg.K)]	840
	Density [kg/m^3]	2130
Green roof	Plant height [m]	0.25
	Leaf area index (LAI) [m^2/m^2]	2.5
	Plant albedo	0.2
Green wall	Plant height [m]	0.25
	Leaf area index (LAI) [m^2/m^2]	2.5
	Plant albedo	0.2
Ground tree	Plant height [m]	8
	Plant width [m]	11
	Leaf area index (LAI) [m^2/m^2]	4
	Plant albedo	0.28
	Foliage transmittance	0.1

the cooling effects of strategies from both spatial and temporal dimensions. Higher CD values for certain hours in dicate that the GI strategy can impact larger areas, while higher cooling hours indicate that the GI strategy can support longer cooling period. Fig. 8 shows that the CD values were dissimilar across the different GI strategies, urban morphology settings, and microclimatic variables.

For the seven GI strategies, similar to CI and CA, Roof exerted negligible impacts on the pedestrian-level microclimate and thermal comfort. Regardless of the outcome variables, the green roof cases showed 0 h of cooling provision. Wall and RoofWall consistently showed low CD values when quantifying by MRT and PET, with only a small

fraction of areas (6%–10%) showing 1 h of cooling in high SVF canyons. However, for AT, Wall and RoofWall showed more evident cooling effects; specifically, 20%–60% of areas were cooled by 0.5 °C for at least 1 h, and at least 4%–7% areas benefited from Wall and RoofWall for 9 h when the SVF was greater than 0.6 in the NS-oriented canyons. These inconsistent results not only indicate the significance of selecting the microclimate variables accordingly, but also justify the necessity to quantify the cooling effects of GI strategies from both spatial and temporal perspectives.

In terms of the impacts of urban morphology, NS and EW orientations had similar CD patterns for different GI strategies and SVF values. EW-oriented canyons yielded more benefits than those with NS orientation, as the CD values for longer hours were relatively higher. For example, when quantified by MRT and applying Tree in canyons (SVF = 0.3), the percentage area cooled for 8 h of CD in EW streets was 45% higher than in NS streets. The difference between the two orientations was more apparent with AT than with MRT and PET, especially for low SVF (0.1–0.5). In terms of SVF, higher SVF values were associated with higher CD at longer cooling periods. This indicates that the GI strategies could play a more significant role in wider and more open street canyons. Streets with SVF = 0.7 benefited the most from GI strategies, as the CD values were the highest for the longer hours, irrespective of the orientation settings or GI strategies. Areas with values of SVF = 0.1 gained the least benefits with more areas showing cooling benefits in 0 h. Furthermore, when implementing trees, above 80% of the areas were cooled for at least 7 h in canyons with SVF = 0.7, but this value was only 2%–20% when SVF = 0.1. Further details are presented in the Supplementary File.

4. Discussion

4.1. The cooling effects of GI strategies

Previous studies predominantly focused on the cooling effects of a single GI typology or the cooling differences between single and combined GI typologies. Based on three typical GI typologies, namely green roof, green wall, and ground trees, seven GI strategies in total can be realized. However, the current evidence does not support cross-

Table A2
The validation results of ENVI-met model (XXX et al., 2022, masked for blind review).

Variable*	Metrics#	Green Roof	Bare Roof	Green Wall	Bare Wall	Ground Tree	Tree Free
AT (°C)	R^2	0.67	0.64	0.93	0.89	0.73	0.62
	d	0.88	0.7	0.89	0.94	0.68	0.82
	RMSE	0.65	1.63	0.56	0.44	0.96	0.73
	MBE	−0.29	−1.34	0.3	−0.2	0.71	0.03
RH (%)	R^2	0.54	0.25	0.76	0.87	0.58	0.13
	d	0.63	0.7	0.6	0.6	0.28	0.42
	RMSE	4.27	3.9	5.15	4.95	8.58	5.84
	MBE	−3.4	−1.15	−4.71	−4.5	−8.15	−4.51
MRT (°C)	R^2	0.79	0.87	0.84	0.62	0.67	0.85
	d	0.87	0.9	0.8	0.88	0.37	0.94
	RMSE	7.49	7.48	9.08	6.93	5.79	5.74
	MBE	5.25	5.82	8.18	1.28	5.55	3.26
SW_{down} (W/m^2)	R^2	0.62	0.86	0.32	0.13	0.3	0.85
	d	0.84	0.94	0.75	0.63	0.32	0.95
	RMSE	227.11	136	335.71	436.68	41.86	142.08
	MBE	136.62	89.51	−153	−231.7	33.12	36.8
SW_{up} (W/m^2)	R^2	0.66	0.81	0.74	0.6	0.08	0.74
	d	0.87	0.94	0.88	0.72	0.52	0.91
	RMSE	23.13	24.71	21.93	49.08	5.41	27.59
	MBE	−11.65	0.04	−14.41	−39.33	3.76	−5.62
LW_{down} (W/m^2)	R^2	0.23	0.22	0.77	0.07	0.04	0.27
	d	0.57	0.42	0.23	0.22	0.09	0.56
	RMSE	8.55	15.72	31.13	24.79	25.83	12.64
	MBE	1.51	14.53	30.94	24.1	24.38	−9.87
LW_{up} (W/m^2)	R^2	0.61	0.94	0.92	0.85	0.39	0.52
	d	0.82	0.65	0.53	0.65	0.11	0.77
	RMSE	15.36	36.39	43.54	31.69	27.68	25.3
	MBE	9.44	−31.67	42.64	30.35	27.43	14.48
LW_{in} (W/m^2)	R^2			0.67	0.88		
	d			0.47	0.25		
	RMSE			10.36	33.05		
	MBE			−9.88	31.25		
LW_{out} (W/m^2)	R^2			0.67	0.51		
	d			0.38	0.84		
	RMSE			40.67	10.98		
	MBE			−38.75	−0.74		

* AT: air temperature; RH: relative humidity; MRT: mean radiant temperature; SW_{down} and SW_{up}: downward and upward shortwave radiation; LW_{down} and LW_{up}: downward and upward longwave radiation; LW_{in} and LW_{out}: incoming and outgoing longwave radiation of the wall;
# R^2: the coefficient of determination; d: the index of agreement; RMSE: the root mean square error; MBE: the mean bias error;

comparisons between those strategies in terms of their cooling performance. Therefore, this study was inspired by this research gap and aimed to compare them systematically.

Regarding single GI typologies, the results in this study indicate that green roof had limited impacts on pedestrian-level microclimate and thermal comfort: the average reductions in AT, MRT, and PET within the analysis domain were 0.00–0.07 °C, 0.00–0.02 °C, and 0.00–0.04 °C, respectively. This finding is in accordance with previous studies showing negligible cooling effects by green roof with 100% coverage ratio in HK and Japan (Chen et al., 2009; Ng et al., 2012). One possible reason for this outcome is that the building heights in this study were set at 10–60 m, but the roof greenery may only benefit the pedestrian level when the building height is lower than 10 m (Wong et al., 2003). Green wall showed slightly higher cooling effects than green roof, especially in terms of nearby ambient temperatures, with reductions ranging from 0.24 to 0.37 °C. This is in line with the findings in a previous parametric study (Alexandri & Jones, 2008). However, this value was lower than that found by another parametric study at the neighbourhood scale in HK, which revealed a ~ 1 °C reduction in AT when using 30–50% of green façade (Morakinyo et al., 2019). The possible reason for this difference is that the updated version of ENVI-met enables the modelling of multiple façade layers, including green wall, while the previous version could only use 1-dimensional greening to represent the green wall (Ouyang et al., 2022, masked for blind review). Furthermore, this study also unveiled that green wall may increase MRT in narrow canyons, as a 0.44–1.84 °C increase in MRT was found in canyons with SVF = 0.1 and SVF = 0.2. One possible explanation is that the radiation balance is dominated by longwave radiation in narrow canyons, as shortwave

radiation is blocked by the buildings and, thus penetrates less to the pedestrian level (Ge et al., 2022). Therefore, the longwave radiation trapper by both leaves and canyons may slightly increase the MRT (Oke, 1981). When GI strategies involved trees, the cooling benefits were greatly improved. For example, trees (30% coverage for the whole simulation domain), on average, reduced AT by 0.46–1.10 °C, MRT by 4.63–16.49 °C, and PET by 2.12–9.03 °C. The cooling effects were slightly higher than in other studies in Hong Kong where 34% tree coverage produced a 0.2–0.7 °C reduction in AT (Ng et al., 2012), 30% tree coverage lead to 0.7–0.9 °C reduction in AT, 6 °C reductions in MRT, 2.5 °C reductions in PET (Ouyang et al., 2020, masked for blind review). These differences may be due to the different simulation scales (street canyon vs. neighbourhood), building morphology settings, and meteorological inputs.

Regarding the combined GI strategies, this study found that utilizing the three GI typologies simultaneously did not always lead to the highest cooling benefits. For instance, the RoofWallTree strategy showed the highest cooling effects in AT across all morphological settings (0.62–1.41 °C) but yielded slightly lower cooling benefits in terms of MRT (3.29–15.97 °C) compared to the Tree strategy (4.63–16.49 °C) and RoofTree strategy (4.64–16.53 °C). This may partly be due to the warming effects of green wall discussed previously (Djedjig et al., 2017; Lee & Jim, 2019) and the possible effects of overlapping leaves (Cameron et al., 2014). Additionally, this finding was inconsistent with a previous study, which found that combining grass, tree, and green roof showed the higher cooling effects than only combining grass and trees (15.03–20.65 °C vs. 7.84–15.57 °C in MRT, 5.68–6.94 °C vs. 4.47–6.7 °C in PET) (Lobaccaro & Acero, 2015). It should be noted that the GI

Table A3

Post-hoc results of the one-way ANOVA.

GI pair	AT		MRT		PET	
	Diff	p-value adj	Diff	p-value adj	Diff	p-value adj
Wall – Roof	−0.28	0.00	−0.41	0.00	−0.41	0.00
Tree – Roof	−0.71	0.00	−11.77	0.00	−6.08	0.00
RoofWall – Roof	−0.30	0.00	−0.41	0.00	−0.41	0.00
RoofTree – Roof	−0.72	0.00	−11.78	0.00	−6.09	0.00
WallTree – Roof	−0.87	0.00	−11.27	0.00	−5.97	0.00
RoofWallTree – Roof	−0.88	0.00	−11.28	0.00	−5.98	0.00
Tree – Wall	−0.43	0.00	−11.37	0.00	−5.67	0.00
RoofWall – Wall	−0.02	0.00	0.00	1.00	0.00	1.00
RoofTree – Wall	−0.44	0.00	−11.38	0.00	−5.68	0.00
WallTree – Wall	−0.58	0.00	−10.86	0.00	−5.56	0.00
RoofWallTree – Wall	−0.60	0.00	−10.87	0.00	−5.57	0.00
RoofWall – Tree	0.41	0.00	11.36	0.00	5.67	0.00
RoofTree – Tree	−0.01	0.00	−0.01	1.00	−0.01	0.98
WallTree – Tree	−0.16	0.00	0.51	0.00	0.11	0.00
RoofWallTree – Tree	−0.17	0.00	0.50	0.00	0.10	0.00
RoofTree – RoofWall	−0.43	0.00	−11.37	0.00	−5.68	0.00
WallTree – RoofWall	−0.57	0.00	−10.86	0.00	−5.56	0.00
RoofWallTree – RoofWall	−0.58	0.00	−10.87	0.00	−5.57	0.00
WallTree – RoofTree	−0.14	0.00	0.51	0.00	0.12	0.00
RoofWallTree – RoofTree	−0.16	0.00	0.51	0.00	0.11	0.00
RoofWallTree – WallTree	−0.01	0.00	−0.01	1.00	−0.01	0.99

strategy settings were dissimilar in this study. Additionally, the simulation model versions and building morphologies were also different. Therefore, direct comparisons of the values should be undertaken with cautions. This difficulty in direct cross-comparison justifies the necessity of the systematic comparison of GI strategies in this study.

4.2. The spatio-temporal perspective

Current discussions lack a spatio-temporal perspective regarding the cooling effects in parametric studies. For instance, most recent studies have only reported the average or maximum cooling effects at the hottest hour (i.e., 14:00). Therefore, this study appllied three cooling indicators to assess the cooling effects: cooling intensity (CI), which describes the average cooling capacity for a certain area or period; cooling area (CA), which measures the cooling impact areas from the spatial perspective; and cooling duration (CD), which indicates the cooling hours and impact areas from the spatio-temporal perspective.

The results indicated that seven GI strategies showed consistent patterns of the cooling effects, regardless of the different cooling indicators. The Wall strategy showed the least cooling effects, followed by the Roof and RoofWall strategies; when involving trees, cooling effects were idnetified apparently for all three variables. RoofWallTree achieved the highest cooling effects when quantified by AT, while RoofTree provided the greatest cooling in terms MRT and PET (see Figs. 4 & 5). When investigating the details for different variables (i.e., AT, MRT, and PET), these three cooling effect indicators showed dissimilar patterns. CI is the most used indicator in previous studies, whose results have been discussed in section 4.1. Regarding CA, the range values were similar between AT and MRT, and these values were slightly higher than those of PET. For instance, the Tree strategy applied in different SVF settings presented 41%–87% and 42%–90% CA for AT and MRT respectively, but showed 14%–85% CA for PET, meaning trees can cool 41%–87% of canyon areas for at least 0.5 °C in AT, and 42%–90% areas for at least 5 °C in MRT, and 14%–85% areas for at least 4 °C in PET. In terms of CD,

Table A4

The detailed results of cooling intensity (CI) *unit:* °C.

Variable	SVF	NS orientation							EW orientation						
		Roof	Wall	Tree	RoofWall	RoofTree	WallTree	RoofWallTree	Roof	Wall	Tree	RoofWall	RoofTree	WallTree	RoofWallTree
AT	0.1	0.00	−0.28	−0.46	−0.28	−0.46	−0.62	−0.62	0.00	−0.32	−0.45	−0.32	−0.45	−0.62	−0.63
	0.2	0.00	−0.24	−0.56	−0.24	−0.56	−0.70	−0.70	0.00	−0.33	−0.65	−0.33	−0.65	−0.83	−0.83
	0.3	0.00	−0.26	−0.54	−0.26	−0.54	−0.69	−0.69	0.00	−0.29	−0.60	−0.29	−0.60	−0.77	−0.77
	0.4	0.00	−0.29	−0.61	−0.29	−0.61	−0.77	−0.77	0.00	−0.31	−0.67	−0.31	−0.67	−0.85	−0.85
	0.5	0.00	−0.34	−0.76	−0.35	−0.76	−0.95	−0.95	0.00	−0.34	−0.86	−0.34	−0.86	−1.05	−1.05
	0.6	0.00	−0.30	−0.63	−0.30	−0.63	−0.79	−0.79	0.00	−0.28	−0.68	−0.29	−0.69	−0.85	−0.85
	0.7	−0.07	−0.37	−1.10	−0.44	−1.17	−1.26	−1.32	−0.07	−0.34	−1.19	−0.40	−1.25	−1.34	−1.41
	0.8	−0.05	−0.28	−0.86	−0.33	−0.91	−0.97	−1.02	−0.05	−0.25	−0.86	−0.30	−0.91	−0.97	−1.02
MRT	0.1	0.00	1.84	−4.63	1.84	−4.64	−3.29	−3.29	0.00	1.73	−4.83	1.73	−4.83	−3.49	−3.49
	0.2	0.00	0.44	−8.19	0.44	−8.19	−7.48	−7.48	0.00	−0.17	−9.62	−0.17	−9.62	−8.96	−8.96
	0.3	0.00	−0.30	−9.36	−0.29	−9.38	−8.94	−8.95	0.00	−0.36	−10.35	−0.35	−10.36	−9.91	−9.91
	0.4	0.00	−0.65	−10.67	−0.65	−10.65	−10.30	−10.27	0.00	−0.47	−11.53	−0.47	−11.53	−11.11	−11.11
	0.5	0.00	−0.92	−12.39	−0.92	−12.39	−11.94	−11.95	0.00	−0.57	−13.58	−0.57	−13.58	−13.12	−13.12
	0.6	0.00	−0.98	−11.50	−0.98	−11.50	−11.20	−11.20	0.00	−0.55	−12.09	−0.55	−12.10	−11.76	−11.76
	0.7	−0.02	−1.10	−16.49	−1.12	−16.53	−15.93	−15.97	−0.02	−0.64	−17.30	−0.66	−17.34	−16.73	−16.77
	0.8	−0.02	−0.87	−14.49	−0.89	−14.52	−14.11	−14.14	−0.02	−0.51	−14.65	−0.53	−14.68	−14.25	−14.28
PET	0.1	0.00	0.53	−2.12	0.54	−2.13	−1.67	−1.67	0.00	0.46	−2.18	0.46	−2.18	−1.74	−1.74
	0.2	0.00	−0.01	−3.78	−0.01	−3.78	−3.57	−3.57	0.00	−0.34	−4.45	−0.34	−4.45	−4.31	−4.30
	0.3	0.00	−0.33	−4.40	−0.33	−4.41	−4.32	−4.32	0.00	−0.41	−4.93	−0.40	−4.93	−4.86	−4.86
	0.4	0.00	−0.52	−5.09	−0.51	−5.08	−5.05	−5.03	0.01	−0.49	−5.67	−0.48	−5.67	−5.62	−5.61
	0.5	0.01	−0.68	−6.16	−0.67	−6.16	−6.09	−6.09	0.01	−0.56	−6.97	−0.55	−6.96	−6.90	−6.90
	0.6	0.01	−0.70	−5.94	−0.69	−5.93	−5.92	−5.92	0.01	−0.50	−6.39	−0.49	−6.39	−6.36	−6.36
	0.7	−0.04	−0.73	−9.03	−0.76	−9.09	−8.88	−8.94	−0.04	−0.42	−9.50	−0.45	−9.56	−9.36	−9.42
	0.8	−0.03	−0.57	−8.34	−0.60	−8.38	−8.24	−8.29	−0.02	−0.31	−8.42	−0.33	−8.46	−8.32	−8.37

Table A5
The detailed results of cooling area (CA) *unit: %.*

Variable	SVF	NS orientation							EW orientation						
		Roof	Wall	Tree	RoofWall	RoofTree	WallTree	RoofWallTree	Roof	Wall	Tree	RoofWall	RoofTree	WallTree	RoofWallTree
AT	0.1	0.00	11.56	40.56	11.78	40.67	55.33	55.44	0.00	11.56	41.44	11.89	41.67	61.11	61.33
	0.2	0.00	7.44	47.44	7.44	47.56	59.00	59.00	0.00	20.33	61.44	20.44	61.56	71.78	71.78
	0.3	0.00	12.89	48.33	12.89	48.44	60.44	60.44	0.00	16.11	49.89	16.00	49.78	63.00	62.89
	0.4	0.00	17.00	55.44	17.11	55.44	66.22	66.11	0.00	17.56	62.22	17.44	62.11	74.22	74.00
	0.5	0.00	23.78	68.22	24.33	68.22	76.11	76.11	0.00	22.44	81.33	23.33	81.22	86.22	86.11
	0.6	0.00	18.78	55.56	19.22	55.44	66.11	66.00	0.00	16.44	65.67	16.89	65.56	74.33	74.33
	0.7	0.00	27.00	86.89	38.22	87.44	89.44	89.67	0.00	20.00	90.78	33.44	90.67	92.56	92.56
	0.8	0.00	15.56	80.11	22.44	80.78	84.00	85.22	0.00	11.67	79.78	18.78	80.33	82.89	83.00
MRT	0.1	0.00	0.00	42.33	0.00	42.33	30.67	30.78	0.00	0.00	39.78	0.00	39.78	30.00	30.00
	0.2	0.00	0.00	71.89	0.00	71.89	65.11	65.11	0.00	0.00	79.67	0.00	79.67	75.11	75.11
	0.3	0.00	0.00	79.33	0.00	79.33	76.22	76.33	0.00	0.00	81.67	0.00	81.67	78.78	78.67
	0.4	0.00	0.00	81.89	0.00	81.89	80.33	80.22	0.00	0.00	84.89	0.00	84.89	82.22	82.22
	0.5	0.00	0.67	86.56	0.67	86.67	84.67	84.67	0.00	0.00	87.11	0.00	87.11	84.67	84.67
	0.6	0.00	1.11	86.56	1.11	86.56	85.11	85.11	0.00	0.00	86.56	0.00	86.56	85.33	85.33
	0.7	0.00	0.78	89.67	0.78	89.67	87.11	87.44	0.00	0.00	89.67	0.00	89.78	87.89	87.89
	0.8	0.00	0.00	89.56	0.00	89.78	88.78	89.00	0.00	0.00	88.44	0.00	88.56	88.33	88.44
PET	0.1	0.00	0.00	13.89	0.00	14.00	11.67	11.67	0.00	0.00	13.67	0.00	13.67	11.78	11.78
	0.2	0.00	0.00	43.67	0.00	43.78	40.33	40.44	0.00	0.00	57.00	0.00	57.00	56.78	56.78
	0.3	0.00	0.00	56.22	0.00	56.78	54.44	54.56	0.00	0.11	56.67	0.11	56.78	56.33	56.33
	0.4	0.00	0.00	65.89	0.00	65.44	66.56	65.89	0.00	0.11	70.56	0.11	70.56	69.56	69.44
	0.5	0.00	0.11	72.33	0.11	72.22	72.11	72.11	0.00	0.11	79.11	0.22	79.11	78.44	78.56
	0.6	0.00	0.33	70.67	0.33	70.67	70.00	70.00	0.00	0.33	76.11	0.22	76.00	75.22	75.22
	0.7	0.00	1.67	84.56	1.89	84.78	83.89	84.22	0.00	0.00	87.56	0.00	87.56	86.89	87.11
	0.8	0.00	1.11	84.11	1.33	84.44	82.89	83.11	0.00	0.33	83.89	0.44	84.22	83.11	83.22

the patterns of MRT and PET were quite similar, but were different from that of AT. For example, in NS-oriented canyons and with SVF = 0.7, the Tree strategy cooled 49% of areas for 9 h for AT, but this value was only 1% for MRT and 0% for PET. These differences may partially be due to the threshold for CA and CD calculations: 0.5 °C for AT, 5 °C for MRT, and 4 °C for PET. The thresholds can be adjusted for different research or practical objectives in other cities. The cooling indicators proposed in this study, such as CA and CD provide a spatio-temporal lens to understand the cooling effects of urban greenery. This perspective not only supports the comprehensive understanding of the cooling effects of GI strategies, but also targets different goals in urban planning and implementation process.

4.3. The impacts of urban morphology on the GI cooling

It is important to examine the impacts of the urban morphology on the cooling provision of GI strategies (Jamei et al., 2016) so that GI strategies can be recommended and tailored for certain neighbourhoods with different morphological characteristics. Therefore, this study modeled urban morphology based on two important factors: street orientation and sky view factor (SVF). The performance of GI strategies in these different morphological settings was cross-compared systematically.

The results revealed that EW oriented canyons benefited more than NS oriented canyons from the GI strategies, especially for those strategies with trees. Higher CI, larger CA, and longer CD were observed in the EW orientation. This is largely because EW-oriented streets endure uncomfortable microclimates for longer than NS-oriented streets due to the EW orientation receiving higher solar radiation in summer, as has been reported in previous studies (Gong et al., 2019; Rodríguez Algeciras et al., 2016). In terms of the SVF, areas with larger SVF usually experienced greater cooling effects, with higher CI, CA, and CD values. One explanation for this pattern is that the building shading effects are stronger in canyons with lower SVF, meaning the cooling effects from the shading from greenery were reduced (Morakinyo et al., 2020; Ouyang et al., 2020, masked for blind review). Therefore, when streets are deep and narrow (SVF = 0.1), it is not recommended to implement the Wall and RoofWall strategies, as this might lead to a slight increase in MRT and PET in the outdoor environment. GI cooling potential was maximally utilized for streets with SVF = 0.7, as the CI, CA, and CD values were all the highest in these areas. However, when the streets are wider (SVF = 0.8), the cooling effects of GI strategies decrease marginally. This finding indicates that extra strategies other than urban greenery should be considered for wider streets, as the cooling provision of GI strategies cannot counterbalance the thermal loads received from the solar radiations in these areas (Santamouris et al., 2017).

4.4. Implications for research and practice

The implications of this study can be discussed in terms of both research and practice. For research in urban climate and urban planning, this study presents a systematic quantification approach to investigating the cooling effects of GI strategies. In the present work, a parametric study in ENVI-met was used to simulate different GI strategies and urban morphological conditions. Subsequently, three cooling indicators were proposed and applied to quantify the cooling effects of those strategies from a spatio-temporal perspective. In the future, the approach and indicators in this study can be applied to other cities and study areas.

As for practices in sustainable planning and design, this study suggests that GI strategies should be selected based on certain morphological conditions and thermal comfort targets, as depicted in Fig. 9. Firstly, it is recommended that trees are utilized as a priority, and this suggestion is in line with the findings of previous studies (Ng et al., 2012; Ouyang et al., 2021, masked for blind review). Secondly, EW-oriented streets need more attention, as they are subject to higher heat stress and gain more benefits from GI strategies. Thirdly, when streets are

narrow or deep (SVF = 0.1 – 0.2), it is not recommended to implement GI strategies, especially green wall at the pedestrian level, as the thermal benefits were found to be minimal and some warming effects may be produced due to longwave radiation trapping within the narrow canyons. However, the green wall may be applicable for the podium or upper parts of towers based on the evidence presented in (Morakinyo et al., 2019). When streets are wide and open with SVF = 0.8, other strategies should be adopted to complement urban greenery for cooling provision. Moreover, the three cooling indicators are of interest concerning street design and its objectives concerning street design and its effects on thermal comfort, as they can be used for different assessment targets. For instance, when planning and designing with the target of providing higher temperature reduction, CI indicator should be used. When underscoring the impact areas that a strategy can cover, CA indicator could be applied. When emphasizing the cooling persistence for both larger areas and longer periods, CD indicator could be considered. The thresholds for the CA and CD calculation should also be tailored based on different cities and objectives.

Specifically, for the local context in Hong Kong, although the Hong Kong government has been encouraging the implementation of urban greenery, the high-density and complex morphological characteristics may prevent urban planners and architects from involving urban greenery in their design schemes. The results of this study provide a strong incentive for planners to consider green wall and green roof in their design schemes. For instance, Hong Kong Planning Standards and Guidelines require each public housing development to achieve 30% green coverage (Planning Department, 2010). If there is limited spaces in the horizontal pedestrian zones to apply greenery, green wall and green roof can be utilized to meet the requirements (Buidling Department, 2014, 2016). Furthermore, this study reminds practitioners to consider the morphological features (i.e., the street orientations and the openness and compactness of the neighbourhoods) before designing or implementing greenery for a site. Therefore, other than the applicable findings in the context of subtropical climate, there is generalizable knowledge that this study may offer beyond the HK city.

4.5. Limitations and future work

This study has several limitations, which represent promising future directions to be explored. Firstly, this study only covered the diurnal periods when downward radiation plays a significant role in the microclimate. As the urban heat island effect is intensified during heatwave events at night (Ren et al., 2021), further studies are warranted to investigate the cooling performance of GI strategies at night. Secondly, to control for the effects of wind conditions, this parametric study set the wind speed as constant at 1 m/s for all simulation periods, and the wind direction was parallel to the street canyon direction. We did a sensitivity test for different wind speeds and directions, and the results showed that the main findings of this study were robust, although with different values for the cooling effects (the details are provided in Supplementary File). Wind conditions are a significant factor for pedestrian-level thermal comfort (Ng et al., 2011), thus meaning it is important to examine the impact of wind on the cooling provision of GI strategies. Thirdly, this study mainly focused on the outdoor thermal environment, but the green roof and green wall strategies also benefit indoor thermal environments and energy-saving (He et al., 2020; Pérez et al., 2014). Therefore, future research should investigate the combination of both the outdoor and indoor benefits of GI strategies. It would be also worth examining and comparing the cooling effects of GI strategies at both street and podium levels (Morakinyo et al., 2020). Furthermore, as climate change will increase the intensity, frequency, and duration of extreme heat in the future (Ren et al., 2021), it is warranted to examine the applicability of current urban design strategies to future scenarios, from the perspectives of both public health (Wang et al., 2019) and energy consumption (Liu et al., 2020).

5. Conclusion

Using parametric studies in ENVI-met, this study assessed the cooling capacity of GI strategies in different urban morphologies in the humid subtropical city of Hong Kong. This study makes three key contributions to the current literature: 1) systematically quantifying the cooling effects of seven GI strategies involving three GI typologies, namely green roof, green wall, and ground tree; 2) proposing to apply three cooling indicators to assess the cooling effects from a spatio-temporal perspective; 3) examining the impacts of urban morphology (i.e., street orientation and SVF) on the cooling provisions of the GI strategies.

The findings can be summarized as follows:

- In terms of GI strategies, strategies involving ground surface GI (i.e., trees) should be prioritized; Indeed, building surface greening contributed limitedly to the outdoor thermal comfort but can decrease the nearby ambient temperature: green wall should be carefully implemented in deep and narrow street canyons, and green roof showed limited cooling for pedestrian thermal comfort at the microclimate scale when applied on high buildings.
- For cooling indicators from a spatio-temporal perspective, cooling intensity (CI) is mostly used for average cooling quantification, while cooling area (CA) is proposed to assess the cooling impact areas, and cooling duration (CD) is proposed to examine the extent of cooling effects on both spatial and temporal scales. These three indicators showed different patterns and can serve different objectives in urban planning and sustainability assessment.
- Regarding the impacts of urban morphology, EW oriented streets received higher cooling effects from GI strategies than NS orientation; Additionally, streets with larger SVF benefited more from GI strategies, and streets with SVF = 0.7 achieved the highest cooling effects. For wider streets (SVF = 0.8), combining urban greenery and other measures for urban heat mitigation should be considered.

This study enhances our understanding of the cooling performance of GI strategies at the pedestrian level across different morphological conditions. Additionally, this study provides a spatio-temporal lens for parametric studies to investigate the cooling effects of different GI strategies. Based on this enhanced knowledge and novel approach, researchers and urban planners can further optimize GI strategies to improve the thermal environment and support urban sustainability.

Declaration of Competing Interest

The authors declare that they have no known competing financial interests or personal relationships that could have appeared to influence the work reported in this paper.

Data availability

Data will be made available on request.

Appendix A

Appendix B. Supplementary data

Supplementary data to this article can be found online at https://doi.

org/10.1016/j.landurbplan.2023.104808.

References

Acero, J. A., Koh, E. J. Y., Li, X., Ruefenacht, L. A., Pignatta, G., & Norford, L. K. (2019). Thermal impact of the orientation and height of vertical greenery on pedestrians in a tropical area. *Building Simulation, 12*(6), 973–984. https://doi.org/10.1007/s12273-019-0537-1

Acero, J. A., Koh, E. J. Y., Ruefenacht, L. A., & Norford, L. K. (2021). Modelling the influence of high-rise urban geometry on outdoor thermal comfort in Singapore. *Urban Climate, 36*, Article 100775. https://doi.org/10.1016/j.uclim.2021.100775

Alexandri, E., & Jones, P. (2008). Temperature decreases in an urban canyon due to green walls and green roofs in diverse climates. *Building and Environment, 43*(4), 480–493. https://doi.org/10.1016/j.buildenv.2006.10.055

Ali-Toudert, F., & Mayer, H. (2006). Numerical study on the effects of aspect ratio and orientation of an urban street canyon on outdoor thermal comfort in hot and dry climate. *Building and Environment, 41*(2), 94–108. https://doi.org/10.1016/j.buildenv.2005.01.013

Arnfield, A. J. (2003). Two decades of urban climate research: A review of turbulence, exchanges of energy and water, and the urban heat island. *International Journal of Climatology, 23*(1), 1–26. https://doi.org/10.1002/joc.859

Berardi, U. (2016). The outdoor microclimate benefits and energy saving resulting from green roofs retrofits. *Energy and Buildings, 121*, 217–229. https://doi.org/10.1016/j.enbuild.2016.03.021

Buidling Department, H. K. S. (2014). *Practice Note for Authorized Persons, Registered Structural Engineers and Registered Geotechnical Engineers APP-151*. 12.

Buidling Department, H. K. S. (2016). *Practice Note for Authorized Persons, Registered Structural Engineers and Registered Geotechnical Engineers APP-152*. 45.

Cameron, R. W. F., Taylor, J. E., & Emmett, M. R. (2014). What's 'cool' in the world of green façades? How plant choice influences the cooling properties of green walls. *Building and Environment, 73*, 198–207. https://doi.org/10.1016/j.buildenv.2013.12.005

Chen, H., Ooka, R., Huang, H., & Tsuchiya, T. (2009). Study on mitigation measures for outdoor thermal environment on present urban blocks in Tokyo using coupled simulation. *Building and Environment, 44*(11), 2290–2299. https://doi.org/10.1016/j.buildenv.2009.03.012

CUHK. (2008). *Urban Climatic Map and Standards for Wind Environment—Feasibility Study* (p. 587). https://www.pland.gov.hk/pland_en/p_study/prog_s/ucmapweb/ucmap_project/content/reports/wp2b.pdf.

Djedjig, R., Belarbi, R., & Bozonnet, E. (2017). Green wall impacts inside and outside buildings: Experimental study. *Energy Procedia, 139*, 578–583. https://doi.org/10.1016/j.egypro.2017.11.256

Fahmy, M., Sharples, S., & Yahiya, M. (2010). LAI based trees selection for mid latitude urban developments: A microclimatic study in Cairo, Egypt. *Building and Environment, 45*(2), 345–357. https://doi.org/10.1016/j.buildenv.2009.06.014

Ge, J., Wang, Y., Akbari, H., & Zhou, D. (2022). The effects of sky view factor on ground surface temperature in cold regions – A case from Xi'an, China. *Building and Environment, 210*, Article 108707. https://doi.org/10.1016/j.buildenv.2021.108707

Gong, F.-Y., Zeng, Z.-C., Ng, E., & Norford, L. K. (2019). Spatiotemporal patterns of street-level solar radiation estimated using Google Street View in a high-density urban environment. *Building and Environment, 148*, 547–566. https://doi.org/10.1016/j.buildenv.2018.10.025

Gong, F.-Y., Zeng, Z.-C., Zhang, F., Li, X., Ng, E., & Norford, L. K. (2018). Mapping sky, tree, and building view factors of street canyons in a high-density urban environment. *Building and Environment, 134*, 155–167. https://doi.org/10.1016/j.buildenv.2018.02.042

He, Y., Yu, H., Ozaki, A., & Dong, N. (2020). Thermal and energy performance of green roof and cool roof: A comparison study in Shanghai area. *Journal of Cleaner Production, 267*, Article 122205. https://doi.org/10.1016/j.jclepro.2020.122205

Herath, H. M. P. I. K., Halwatura, R. U., & Jayasinghe, G. Y. (2018). Evaluation of green infrastructure effects on tropical Sri Lankan urban context as an urban heat island adaptation strategy. *Urban Forestry & Urban Greening, 29*, 212–222. https://doi.org/10.1016/j.ufug.2017.11.013

HK Government. (2021). *Hong Kong's Climate Action Plan 2050*. 66.

HKO. (2019). *Summary of Meteorological and Tidal Observations in Hong Kong*.

HKO. (2020). *Summary of Meteorological and Tidal Observations in Hong Kong*. https://www.hko.gov.hk/tc/publica/smo/files/SMO2020.pdf.

Hong Kong Civil Engineering and Development Department. (2004). *Greening Master Plan*. https://www.cedd.gov.hk/eng/topics-in-focus/greening/index.html.

Huttner, S. (2012). *Further development and application of the 3D microclimate simulation ENVI-met*. Universitätsbibliothek Mainz [PhD Thesis].

IPCC. (2021). *Climate Change 2021: The Physical Science Basis. Contribution of Working Group I to the Sixth Assessment Report of the Intergovernmental Panel on Climate Change*. https://www.ipcc.ch/report/ar6/wg1/.

ISO. (1985). *BS EN ISO 27726:1994—Thermal environments—Instruments and methods for measuring physical quantities*.

Jamei, E., Rajagopalan, P., Seyedmahmoudian, M., & Jamei, Y. (2016). Review on the impact of urban geometry and pedestrian level greening on outdoor thermal comfort. *Renewable and Sustainable Energy Reviews, 54*, 1002–1017. https://doi.org/10.1016/j.rser.2015.10.104

Jin, C., Bai, X., Luo, T., & Zou, M. (2018). Effects of green roofs' variations on the regional thermal environment using measurements and simulations in Chongqing, China. *Urban Forestry & Urban Greening, 29*, 223–237. https://doi.org/10.1016/j.ufug.2017.12.002

Johansson, E. (2006). Influence of urban geometry on outdoor thermal comfort in a hot dry climate: A study in Fez, Morocco. *Building and Environment, 41*(10), 1326–1338. https://doi.org/10.1016/j.buildenv.2005.05.022

Kong, L., Lau, K.-K.-L., Yuan, C., Chen, Y., Xu, Y., Ren, C., & Ng, E. (2017). Regulation of outdoor thermal comfort by trees in Hong Kong. *Sustainable Cities and Society, 31*, 12–25. https://doi.org/10.1016/j.scs.2017.01.018

Lan, H., Lau, K.-K.-L., Shi, Y., & Ren, C. (2021). Improved urban heat island mitigation using bioclimatic redevelopment along an urban waterfront at Victoria Dockside, Hong Kong. *Sustainable Cities and Society, 74*, Article 103172. https://doi.org/10.1016/j.scs.2021.103172

Lee, L. S. H., & Jim, C. Y. (2019). Transforming thermal-radiative study of a climber green wall to innovative engineering design to enhance building-energy efficiency. *Journal of Cleaner Production, 224*, 892–904. https://doi.org/10.1016/j.jclepro.2019.03.278

Liu, S., Kwok, Y. T., Lau, K.-K.-L., Ouyang, W., & Ng, E. (2020). Effectiveness of passive design strategies in responding to future climate change for residential buildings in hot and humid Hong Kong. *Energy and Buildings, 228*, Article 110469. https://doi.org/10.1016/j.enbuild.2020.110469

Liu, Z., Brown, R. D., Zheng, S., Jiang, Y., & Zhao, L. (2020). An in-depth analysis of the effect of trees on human energy fluxes. *Urban Forestry & Urban Greening, 50*, Article 126646. https://doi.org/10.1016/j.ufug.2020.126646

Liu, Z., Cheng, K. Y., He, Y., Jim, C. Y., Brown, RobertD., Shi, Y., … Ng, E. (2022). Microclimatic measurements in tropical cities: Systematic review and proposed guidelines. *Building and Environment, 109411*. https://doi.org/10.1016/j.buildenv.2022.109411

Lobaccaro, G., & Acero, J. A. (2015). Comparative analysis of green actions to improve outdoor thermal comfort inside typical urban street canyons. *Urban Climate, 14*, 251–267. https://doi.org/10.1016/j.uclim.2015.10.002

London Government. (2015, March 16). *Parks and green spaces*. London City Hall. https://www.london.gov.uk//what-we-do/environment/parks-green-spaces-and-biodiversity/parks-and-green-spaces.

Morakinyo, T. E., Dahanayake, K. W. D., Kalani, C., Ng, E., & Chow, C. L. (2017). Temperature and cooling demand reduction by green-roof types in different climates and urban densities: A co-simulation parametric study. *Energy and Buildings, 145*, 226–237. https://doi.org/10.1016/j.enbuild.2017.03.066

Morakinyo, T. E., Lai, A., Lau, K.-K.-L., & Ng, E. (2019). Thermal benefits of vertical greening in a high-density city: Case study of Hong Kong. *Urban Forestry & Urban Greening, 37*, 42–55. https://doi.org/10.1016/j.ufug.2017.11.010

Morakinyo, T. E., Lau, K.-K.-L., Ren, C., & Ng, E. (2018). Performance of Hong Kong's common trees species for outdoor temperature regulation, thermal comfort and energy saving. *Building and Environment, 137*, 157–170. https://doi.org/10.1016/j.buildenv.2018.04.012

Morakinyo, T. E., Ouyang, W., Lau, K.-K.-L., Ren, C., & Ng, E. (2020). Right tree, right place (urban canyon): Tree species selection approach for optimum urban heat mitigation – development and evaluation. *Science of The Total Environment, 719*, Article 137461. https://doi.org/10.1016/j.scitotenv.2020.137461

Ng, E., Chen, L., Wang, Y., & Yuan, C. (2012). A study on the cooling effects of greening in a high-density city: An experience from Hong Kong. *Building and Environment, 47*, 256–271. https://doi.org/10.1016/j.buildenv.2011.07.014

Ng, E., Yuan, C., Chen, L., Ren, C., & Fung, J. C. H. (2011). Improving the wind environment in high-density cities by understanding urban morphology and surface roughness: A study in Hong Kong. *Landscape and Urban Planning, 101*(1), 59–74. https://doi.org/10.1016/j.landurbplan.2011.01.004

Norton, B. A., Coutts, A. M., Livesley, S. J., Harris, R. J., Hunter, A. M., & Williams, N. S. G. (2015). Planning for cooler cities: A framework to prioritise green infrastructure to mitigate high temperatures in urban landscapes. *Landscape and Urban Planning, 134*, 127–138. https://doi.org/10.1016/j.landurbplan.2014.10.018

Oke, T. R. (1981). Canyon geometry and the nocturnal urban heat island: Comparison of scale model and field observations. *Journal of Climatology, 1*(3), 237–254.

Oke, T. R. (1988). Street design and urban canopy layer climate. *Energy and Buildings, 11*(1), 103–113. https://doi.org/10.1016/0378-7788(88)90026-6

Ouyang, W., Morakinyo, T. E., Ren, C., Liu, S., & Ng, E. (2021). Thermal-irradiant performance of green infrastructure typologies: Field measurement study in a subtropical climate city. *Science of The Total Environment, 764*, Article 144635. https://doi.org/10.1016/j.scitotenv.2020.144635

Ouyang, W., Morakinyo, T. E., Ren, C., & Ng, E. (2020). The cooling efficiency of variable greenery coverage ratios in different urban densities: A study in a subtropical climate. *Building and Environment, 174*, Article 106772. https://doi.org/10.1016/j.buildenv.2020.106772

Ouyang, W., Sinsel, T., Simon, H., Morakinyo, T. E., Liu, H., & Ng, E. (2022). Evaluating the thermal-radiative performance of ENVI-met model for green infrastructure typologies: Experience from a subtropical climate. *Building and Environment, 108427*. https://doi.org/10.1016/j.buildenv.2021.108427

Pérez, G., Coma, J., Martorell, I., & Cabeza, L. F. (2014). Vertical Greenery Systems (VGS) for energy saving in buildings: A review. *Renewable and Sustainable Energy Reviews, 39*, 139–165. https://doi.org/10.1016/j.rser.2014.07.055

Planning Department. (2010). *Hong Kong Planning Standards and Guidelines*. https://www.pland.gov.hk/pland_en/tech_doc/hkpsg/index.html.

Qin, H., Cheng, X., Han, G., Wang, Y., Deng, J., & Yang, Y. (2021). How thermal conditions affect the spatial-temporal distribution of visitors in urban parks: A case study in Chongqing, China. *Urban Forestry & Urban Greening, 66*, Article 127393. https://doi.org/10.1016/j.ufug.2021.127393

Ren, C., Wang, K., Shi, Y., Kwok, Y. T., Morakinyo, T. E., Lee, T., & Li, Y. (2021). Investigating the urban heat and cool island effects during extreme heat events in high-density cities: A case study of Hong Kong from 2000 to 2018. *International Journal of Climatology, 41*(15), 6736–6754. https://doi.org/10.1002/joc.7222

Rodríguez Algeciras, J. A., Gómez Consuegra, L., & Matzarakis, A. (2016). Spatial-temporal study on the effects of urban street configurations on human thermal comfort in the world heritage city of Camagüey-Cuba. *Building and Environment, 101*, 85–101. https://doi.org/10.1016/j.buildenv.2016.02.026

Rodríguez-Algeciras, J., Tablada, A., Nouri, A. S., & Matzarakis, A. (2021). Assessing the influence of street configurations on human thermal conditions in open balconies in the Mediterranean climate. *Urban Climate, 40*, Article 100975. https://doi.org/10.1016/j.uclim.2021.100975

Ruth, M., Ghosh, S., Mirzaee, S., & Lee, N. S. (2017). Co-benefits and co-costs of climate action plans for low-carbon cities. In S. Dhakal, & M. Ruth (Eds.), *Creating Low Carbon Cities* (pp. 15–28). Springer International Publishing. https://doi.org/10.1007/978-3-319-49730-3_3.

Salata, F., Golasi, I., de Lieto Vollaro, R., & de Lieto Vollaro, A. (2016). Urban microclimate and outdoor thermal comfort. A proper procedure to fit ENVI-met simulation outputs to experimental data. *Sustainable Cities and Society, 26*, 318–343. https://doi.org/10.1016/j.scs.2016.07.005

Santamouris, M., Ding, L., Fiorito, F., Oldfield, P., Osmond, P., Paolini, R., … Synnefa, A. (2017). Passive and active cooling for the outdoor built environment – Analysis and assessment of the cooling potential of mitigation technologies using performance data from 220 large scale projects. *Solar Energy, 154*, 14–33. https://doi.org/10.1016/j.solener.2016.12.006

Simon, H., Sinsel, T., & Bruse, M. (2020). Introduction of Fractal-Based Tree Digitalization and Accurate In-Canopy Radiation Transfer Modelling to the Microclimate Model ENVI-met. *Forests, 11*(8), 869. https://doi.org/10.3390/f11080869

Singapore Government. (2021). *Singapore Green Plan 2030*. https://www.greenplan.gov.sg/key-focus-areas/overview.

Stewart, I. D. (2011). A systematic review and scientific critique of methodology in modern urban heat island literature. *International Journal of Climatology, 31*(2), 200–217. https://doi.org/10.1002/joc.2141

Tan, Z., Lau, K.-K.-L., & Ng, E. (2016). Urban tree design approaches for mitigating daytime urban heat island effects in a high-density urban environment. *Energy and Buildings, 114*, 265–274. https://doi.org/10.1016/j.enbuild.2015.06.031

Tan, Z., Lau, K.-K.-L., & Ng, E. (2017). Planning strategies for roadside tree planting and outdoor comfort enhancement in subtropical high-density urban areas. *Building and Environment, 120*, 93–109. https://doi.org/10.1016/j.buildenv.2017.05.017

Tan, Z., Wang, A., Morakinyo, T. E., Yung, E. H. K., & Chan, E. H. W. (2022). Assessing the mitigation performance of building setback from street and the combination with roadside tree planting. *Building and Environment*, 108814. https://doi.org/10.1016/j.buildenv.2022.108814

Tsoka, S., Tsikaloudaki, A., & Theodosiou, T. (2018). Analyzing the ENVI-met microclimate model's performance and assessing cool materials and urban vegetation applications–A review. *Sustainable Cities and Society, 43*, 55–76. https://doi.org/10.1016/j.scs.2018.08.009

Unger, J. (2004). Intra-urban relationship between surface geometry and urban heat island: Review and new approach. *Climate Research, 27*(3), 253–264.

van Ommen Kloeke, A. E. E., Douma, J. C., Ordoñez, J. C., Reich, P. B., & van Bodegom, P. M. (2012). Global quantification of contrasting leaf life span strategies for deciduous and evergreen species in response to environmental conditions. *Global Ecology and Biogeography, 21*(2), 224–235. https://doi.org/10.1111/j.1466-8238.2011.00667.x

Wang, D., Lau, K.-K.-L., Ren, C., Goggins, W. B. I., Shi, Y., Ho, H. C., … Ng, E. (2019). The impact of extremely hot weather events on all-cause mortality in a highly urbanized and densely populated subtropical city: A 10-year time-series study (2006–2015). *Science of The Total Environment, 690*, 923–931. https://doi.org/10.1016/j.scitotenv.2019.07.039

Weng, Q. (2009). Thermal infrared remote sensing for urban climate and environmental studies: Methods, applications, and trends. *ISPRS Journal of Photogrammetry and Remote Sensing, 64*(4), 335–344. https://doi.org/10.1016/j.isprsjprs.2009.03.007

Wong, N. H., Chen, Y., Ong, C. L., & Sia, A. (2003). Investigation of thermal benefits of rooftop garden in the tropical environment. *Building and Environment, 38*(2), 261–270. https://doi.org/10.1016/S0360-1323(02)00066-5

Wong, N. H., Tan, A. Y. K., Tan, P. Y., & Wong, N. C. (2009). Energy simulation of vertical greenery systems. *Energy and Buildings, 41*(12), 1401–1408. https://doi.org/10.1016/j.enbuild.2009.08.010

Wong, N. H., Tan, C. L., Kolokotsa, D. D., & Takebayashi, H. (2021). Greenery as a mitigation and adaptation strategy to urban heat. *Nature Reviews Earth & Environment*. https://doi.org/10.1038/s43017-020-00129-5

Wu, Z., & Chen, L. (2017). Optimizing the spatial arrangement of trees in residential neighborhoods for better cooling effects: Integrating modeling with in-situ measurements. *Landscape and Urban Planning, 167*, 463–472. https://doi.org/10.1016/j.landurbplan.2017.07.015

Yin, S., Lang, W., & Xiao, Y. (2019). The synergistic effect of street canyons and neighbourhood layout design on pedestrian-level thermal comfort in hot-humid area of China. *Sustainable Cities and Society, 49*, Article 101571. https://doi.org/10.1016/j.scs.2019.101571

Zhang, G., He, B.-J., Zhu, Z., & Dewancker, B. J. (2019). Impact of morphological characteristics of green roofs on pedestrian cooling in subtropical climates. *International Journal of Environmental Research and Public Health, 16*(2), 179. https://doi.org/10.3390/ijerph16020179

Zhao, Q., Sailor, D. J., & Wentz, E. A. (2018). Impact of tree locations and arrangements on outdoor microclimates and human thermal comfort in an urban residential environment. *Urban Forestry & Urban Greening, 32*, 81–91. https://doi.org/10.1016/j.ufug.2018.03.022

Ziaul, S., & Pal, S. (2020). Modeling the effects of green alternative on heat island mitigation of a meso level town, West Bengal, India. *Advances in Space Research, 65*(7), 1789–1802. https://doi.org/10.1016/j.asr.2019.12.031

Ziter, C. D., Pedersen, E. J., Kucharik, C. J., & Turner, M. G. (2019). Scale-dependent interactions between tree canopy cover and impervious surfaces reduce daytime urban heat during summer. *Proceedings of the National Academy of Sciences, 116*(15), 7575–7580. https://doi.org/10.1073/pnas.1817561116

Zölch, T., Maderspacher, J., Wamsler, C., & Pauleit, S. (2016). Using green infrastructure for urban climate-proofing: An evaluation of heat mitigation measures at the micro-scale. *Urban Forestry & Urban Greening, 20*, 305–316. https://doi.org/10.1016/j.ufug.2016.09.011